Ukrainian Journal of Physical Optics
ISSUE 3
2026

SOLITON PROPAGATION, MODULATION, AND STABILITY ANALYSIS OF FRACTIONAL NONLINEAR OPTICAL MODELS: A CONFORMABLE DERIVATIVE APPROACH

WAEL W. MOHAMMED [1,2], MD. TIPU SULTAN [3], DOAA RIZK [4,*] AND M. ALI AKBAR [5,6]

[1] Department of Mathematics, College of Science, University of Ha'il, Ha'il 2440, Saudi Arabia
[2] Department of Mathematics, Faculty of Science, Mansoura University, Mansoura 35516, Egypt
[3] Department of Applied Mathematics, Gono Bishwabidyalay, Savar, Dhaka, Bangladesh
[4] Department of Mathematics, College of Science, Qassim University, Saudi Arabia
[5] Miyan Research Institute, International University of Business Agriculture and Technology, Dhaka, Bangladesh
[6] Department of Applied Mathematics, University of Rajshahi, Saudi Arabia
* Corresponding author: d.hussien@qu.edu.s

Received: 20.03.2026

Abstract. In this article, we establish a wide class of exact soliton solutions to the Kudryashov generalized nonlinear refractive index equation and the fractional complex Ginzburg-Landau equation. The fractional derivative provides a general mathematical framework for modeling complex dispersive and nonlinear effects in optical media. Its exact solutions help in understanding the qualitative features of wave propagation, such as stability and localization. The conformable derivative framework confirms mathematical reliability and physical applicability in modeling fractional-order dispersion and nonlinear effects. The sine-Gordon expansion (SGE) approach is used within the conformable fractional derivative framework to systematically analyze the models. The approach yields a broad spectrum of analytical solutions, including bell-shaped, anti-bell, kink, breather, cusp, W-shaped, parabolic, and singular solitons. The results show that the wave parameters, such as wave frequency, soliton shape, and amplitude, are well described by fractional order α. They provide insight into the pulse propagation and waveform characteristics in nonlinear media. Graphical representations, including two- and three-dimensional visualizations and contour plots, illustrate the amplitude, phase interplay, and structural transitions between soliton families. This study demonstrates that the SGE approach effectively generates exact solutions for fractional nonlinear evolution equations relevant to nonlinear fiber optics and other systems with complex wave interactions.

Keywords: Fractional derivative, simulation, optical solitons, nonlinear refractive index, complex Ginzburg-Landau equation, sine-Gordon expansion method
UDC: 517.958; 530.145; 517.977; 517.955
DOI: 10.3116/16091833/Ukr.J.Phys.Opt.2026.03041

Introduction

Fractional derivatives extend classical derivatives to non-integer orders and naturally include memory and non-local effects into models of wave propagation. These features are crucial in complex optical media where past field evolution and spatially distributed interactions significantly influence soliton dynamics. This generalization implies that all models are fractional. The nonlinear fractional Schrödinger and related models provide a more realistic description of dispersive, fractal-like, and anomalous dispersive optical media than the classical model. As a result, these equations support a broader class of optical soliton solutions with controllable amplitude, width, and stability. Recent studies employed various fractional operators, such as the conformable, beta, M-fractional, and Atangana-Baleanu derivatives, to obtain exact analytic soliton solutions in optical fibers, metamaterials-based couplers, and time-fractional higher-order systems. These

investigations demonstrate that the characteristics of soliton propagation, such as amplitude, width, and velocity, depend on system parameters, and that fractional-order theory provides a flexible framework for describing the model. These developments highlight the importance of fractional calculus in improving the theory and applications of optical communications and nonlinear photonics. Optical solitons have attracted significant attention from researchers in mathematics, engineering, and physics due to their inherent stability and well-localized structures. These properties make them significant in diverse applications, including nonlinear optics, Bose-Einstein condensates, water-wave dynamics, biophysics, nanoelectromechanical and microelectromechanical systems, Josephson junctions, granular crystals, and solid waveguides. Thus, many mathematicians and researchers have developed various methods and techniques to obtain analytical and numerical soliton solutions for these models. For example, the modified Kudryashov scheme [1], the q-homotopy analysis technique [2], the sine-Gordon and the rational sine-Gordon expansion approach [3, 4], the tanh-coth method [5], the Hirota bilinear scheme [6], the improved Bernoulli sub-equation function procedure [7], the directed extended Riccati method and the generalized Riccati equation technique [8, 9], the new Kudryashov extension technique [10], the mapping method [11], the modified extended direct algebraic process [12], the $(G'/G,1/G)$-expansion approach [13], the finite difference method [14], the localized meshless technique [15, 16], the collocation technique and deep learning method [17, 18], etc.

In fiber optics and optoelectronics, soliton dynamics has significantly transformed telecommunications and precision measurement technologies. Numerous results from this theory are now being applied across a wide range of practical systems [19-24]. Consequently, researchers from various disciplines have proposed several novel concepts. These developments include diverse solitonic structures, such as pure cubic solitons, highly dispersive solitons, Bragg grating configurations, and cubic-quartic solitons, among others [25, 26]. The standard cubic nonlinear Schrödinger equation (NLSE) with Kerr (cubic) nonlinearity describes self-phase modulation (SPM). El-Sheikh, et al [27] considered the fractional model of the nonlinear Schrödinger equation (SNLE) with the Kudryashov generalized refractive index of nonlinear form. This includes the effect of the full intensity as well as the effect of the perturbation term. The model is structured as presented in [27]:

$$\begin{aligned}&\left(\frac{b_1}{|u|^{4n}}+\frac{b_2}{|u|^{3n}}+\frac{b_3}{|u|^{2n}}+\frac{b_4}{|u|^{n}}+b_5|u|^{n}+b_7|u|^{3n}+b_6|u|^{2n}+b_8|u|^{4n}\right)u+iD_t^{\alpha}u+aD_{xx}^{2\alpha}u\\&=i\left(\lambda D_x^{\alpha}\left(u|u|^{2m}\right)+\theta D_x^{\alpha}\left(|u|^{2m}\right)u+\mu|u|^{2m}D_x^{\alpha}u\right)\end{aligned}. \quad (1)$$

Here, m is the strength index of the nonlinearity (when $m=1$, it recovers the classical cubic self-steepening). Physically, it causes the pulse peak to steepen on the trailing edge due to intensity-dependent group velocity, n is the exponent for nonlinear power behavior with $0<n\le 1/2$, b_k (where $k=1,\ 2,\ 3,...,8$) are the constant coefficients of nonlinearity, and a is the chromatic dispersion. θ and μ are introduced as the coefficients for higher-order and nonlinear dispersion effects, respectively. The operators $D_t^{\alpha}u$, $D_x^{\alpha}u$, and $D_{xx}^{2\alpha}u$ represent the conformable fractional derivative with respect to time t and spatial coordinate x of order α and 2α, respectively, with $0<\alpha\le 1$.

Elsherbeny et al. [28] investigated the classical form of the equation (1) through the modified Jacobi elliptic function method and the extended auxiliary equation method. Besides, a number of researchers have recently extensively explored the integer or fractional versions of this model. Murad et al. [29] used the Kudryashov approach to construct various optical soliton solutions of the fractional time-space Schrödinger nonlinear equation, incorporating a Kudryashov-type arbitrary refractive index and two distinct nonlocal nonlinearities. Rizvi et al. [30] analyzed optical soliton formations of the Biswas-Milovic coupled nonlinear equations by using the extended modified auxiliary equation mapping technique. Elsherbeny et al. [31] applied the generalized integration approach to derive optical soliton solutions for the dispersive model with an arbitrary refractive index. Fahad et al. [32] exploited the new mapping technique to develop novel soliton solutions to fractional nonlinear Kudryashov's equation, using beta fractional order derivative and *M*-truncated fractional derivative. Murad et al. [33] made use of the Kudryashov auxiliary equation scheme and the modified tanh expansion scheme to derive the optical soliton solutions for the fractional nonlinear Schrödinger equation.

Wave dynamics in optical transmission lines are commonly described by the fractional complex Ginzburg-Landau (FCGL) equation, which effectively captures the underlying physical processes. It has been shown to be highly effective in analyzing optical solitons in optical transmission systems. By employing the finite-bandwidth idea [34], Newell and Whitehead proposed the complex Ginzburg-Landau equation. Weitzner and Zaslavsky [35] introduced the Ginzburg-Landau fractional complex model. In various studies on nonlinear optics, the FCGL model has been used successfully. We assumed the following space-time Ginzburg-Landau complex fractional equation [36, 37]:

$$iD_t^{\alpha}\phi + aD_x^{2\alpha}\phi + bH\left(|\phi|^2\right)\phi = \frac{1}{|\phi|^2\phi^*}\left[\nu|\phi|^2 D_{xx}^{2\alpha}|\phi|^2 - \beta\left(D_x^{\alpha}|\phi|^2\right)^2\right] + \delta\phi, \qquad (2)$$

where $\phi(x,t)$ denotes a complex-valued function of the spatial coordinate *x* and the temporal coordinate t, respectively, ϕ^* denotes the complex conjugate of ϕ, ensuring consistency with physics. $H\left(|\phi|^2\right)$ s the nonlinear term that describes how the refractive index of the optical medium depends on the light intensity. For different choices of H model, different types of optical nonlinearities, such as for $H(s)=s$ gives gives the standard Kerr nonlinearity $|\phi|^2\phi$, for $H(s)=s^p$ gives the power law nonlinearity, for $H(s)=s+ks^2$ gives the parabolic nonlinearity, etc. The parameters *a* and *b* correspond to the group velocity dispersion and nonlinearity, whereas the coefficients ν and β are real parameters that control the strength of two specific higher-order nonlinear dispersive terms, and δ denotes the detuning coefficient. The operators D_t^{α}, D_x^{α}, and $D_{xx}^{2\alpha}$ represent the fractional conformable order derivatives with respect to time *t* and the spatial coordinate *x* of orders α and 2α, respectively, with $0<\alpha\leq 1$. Eq. (2) is a variant of the Schrödinger nonlinear equation that governs the dynamics of pulse propagation through an optical fiber. In [37], Huang et al. studied the time-space FCGL equation for nonlinearities of the Kerr and power-law cases via the complete discrimination system method. Akram et al. [38] considered the FCGL equation by employing the generalized

projective Riccati equation method. Siddique et al. [39] construct the soliton solutions to the FCGL equation by using the modified $\left(G'/G^2\right)$ and $\left(1/G'\right)$-expansion approach. Leta et al. [40] utilized the bifurcation approach to investigate soliton solutions of the conformable complex Ginzburg-Landau equation. Murad et al. [41] analyzed the optical soliton behaviors arising from the time-fractional Ginzburg-Landau equation with Kerr-type nonlinearity by applying the modified sub-equation technique. Akram et al. [42] construct soliton solutions and apply the new extended ϕ^6-model expansion approach to study the FCGL equation with the Kerr-law nonlinearity for fractional operators of multiple variants. Zafar et al. [43] obtained dark, bright, kink, and W-shaped solitons of the FCGL equation using the modified Exp-function and Kudryashov approaches. Sadaf et al. [44] obtained the periodic, singular, complexiton, dark, and bright solitons of the GLFC model with Kerr law nonlinearity by employing an improved $\tan\left(\psi\left(\zeta\right)/2\right)$-expansion scheme. This study examines the FCGL equation in the context of optical fibers with power-law nonlinearity. The SGE technique has become an effective analytical tool for studying precise solitary wave solutions to fractional and standard nonlinear evolution equations (NLEEs) in mathematical physics and engineering. This analytical technique has proven effective in generating traveling and optical soliton wave solutions to numerous nonlinear models, such as the Fokas-Lenells equation [45], the fractional Wazwaz-Benjamin-Bona-Mahony (WBBM) equation [46], the Tzitzéica-type equations arising in nonlinear optics [47], the conformable time-fractional regularized long wave (RLW) equation [48], the Klein-Gordon equation [49], the space-time fractional nonlinear Schrödinger type models in (1+1)-dimensions [50], etc.

Thus, it is observed that the former studies have investigated integer-order and certain fractional forms of the nonlinear Schrödinger Eq. (1) using the modified Kudryashov scheme, q-homotopy analysis, tanh-coth method, extended auxiliary equation approaches, etc. Also, studies on the space-time fractional complex Ginzburg-Landau Eq. (2) have been carried out using the generalized projective Riccati equation, modified exp-function, bifurcation methods for Kerr or power-law nonlinearities, etc. However, these equations have not yet been examined using the SGE approach in the conformable fractional framework. Moreover, the combined effects of fractional-order derivative, generalized nonlinearity parameters, and dispersion coefficients on soliton shapes have not been fully studied. In particular, transitions among bell-shaped, kink, breather, cusp-like, and W-shaped solitons remain unexplored within a unified analytical framework. This absence limits the understanding of how fractional operators modulate wave stability, phase evolution, and structural diversity in advanced photonic and nonlinear optical systems. Therefore, the objective of this article is to address these gaps by means of the sine-Gordon expansion approach to the conformable fractional Kudryashov generalized nonlinear refractive index model and the fractional complex Ginzburg-Landau equation. The study also aims to systematically construct a broad spectrum of exact and stable optical soliton solutions, including periodic, singular-periodic, parabolic, breather, bell-shaped, anti-bell-shaped, kink, and cusp-like structures. This study also pursues the role of fractional order, wave frequency, and nonlinear parameters in modulating soliton dynamics. This analysis provides deeper physical insight into optical pulse propagation in nonlinear and nonlocal photonic systems. The key contributions of this study are to:

- Explore new and assorted soliton solutions,
- Study the effect of fractional order on soliton dynamics,
- Study analytically and graphically the fractional optical systems,
- The sine-Gordon expansion method is put in use to demonstrate its efficacy and expand its range of applicability.

In this article, we define the conformable fractional order derivative in Section 2. In Section 3, the sine-Gordon expansion method has been discussed. In Section 4, the method has been implemented for some solutions of Kudryashov's form of generalized fractional nonlinear refractive index model and FCGL equation. In section 5, graphical descriptions and discussions are presented. Finally, in Section 6, the conclusion is presented.

Conformable fractional derivative

Khalil *et al*. [51] introduced a new formulation of fractional derivative, referred to as the conformable fractional derivative (CFD), and explored its mathematical properties. This derivative satisfies several differentiation rules, namely the Leibniz, chain, product, power, and quotient rules, making it a well-structured and consistent operator.

Definition: Let us assume $h(x)$ is a function defined from $[0,\infty)$ into $\mathbb{R}$; then the CFD of order α relative to the variable x is defined as follows:

$$\mathcal{D}_x^{\alpha}\left(h(x)\right)=\lim_{\varepsilon\to 0}\frac{h\left(x+\varepsilon x^{1-\alpha}\right)-h(x)}{\varepsilon},\ \text{for all } x>0 \text{ and } 0<\alpha\le 1.$$

Theorems on CFD: Consider $0<\alpha\le 1$, and $u(x)$, $v(x)$ be α -differential at the point $x>0$ and p, q are real parameters. Then the following theorem holds:

(1) $\mathcal{D}_x^{\alpha}\left(pu+qv\right)=p\mathcal{D}_x^{\alpha}\left(u\right)+q\mathcal{D}_x^{\alpha}\left(v\right)$.

(2) $\mathcal{D}_x^{\alpha}\left(u(x)\right)=x^{1-\alpha}\frac{du}{dx}$.

(3) $\mathcal{D}_x^{\alpha}\left(uv\right)=u\mathcal{D}_x^{\alpha}\left(v\right)+v\mathcal{D}_x^{\alpha}\left(u\right)$.

(4) $\mathcal{D}_x^{\alpha}\left(k\right)=0$, where k is constant.

(5) $\mathcal{D}_x^{\alpha}\left(\frac{u}{v}\right)=\frac{v\mathcal{D}_x^{\alpha}\left(u\right)-u\mathcal{D}_x^{\alpha}\left(v\right)}{v^2}$.

(6) $\mathcal{D}_x^{\alpha}\left((uov)(x)\right)=\mathcal{D}_x^{\alpha}\left((uov)(x)\right)v'(x)$.

(7) $\mathcal{D}_x^{\alpha}\left(x^k\right)=kx^{k-\alpha}$, $\forall\ k\in\mathbb{R}$.

Theorems (1-7) can be proved directly, and each is satisfied under the conformable fractional derivative framework.

Description of the SGE method

Let us consider the standard form of the sine-Gordon fractional equation of two variables, y and t, as follows [46-48]:

$$\mathcal{D}_y^{2\alpha}g-\mathcal{D}_t^{2\alpha}g=A^2\sin(g),\tag{3}$$

where A is a constant. The suitable fractional form of the function $g(y,t)=Q(\psi)$, where the wave transformation $\psi=a\frac{y^{\alpha}}{\alpha}+c\frac{t^{\alpha}}{\alpha}$, converts the fractional form of the sine-Gordon

equation into a one-dimensional form of the following:

$$\frac{d^2Q}{d\xi^2}=\frac{A^2}{a^2-c^2}\sin(Q), \tag{4}$$

where c is the velocity of the traveling wave. Some simplification leads to the following equation

$$\left(\frac{d}{d\psi}\left(\frac{Q}{2}\right)\right)^2=\frac{A^2}{a^2-c^2}\sin^2\left(\frac{Q}{2}\right)+f, \tag{5}$$

where f is the integration constant. For simplicity, let us assume that $f=0$, $W(\psi)=Q(\psi)/2$, and $\frac{A^2}{a^2-c^2}=1$. Then equation (5) is converted to

$$\frac{dW}{d\psi}=\sin(W(\psi)). \tag{6}$$

Eq. (6) gives the following relations

$$\sin(W(\psi))=\frac{2re^{\psi}}{r^2e^{2\psi}+1}=\operatorname{sech}(\psi), \tag{7}$$

or

$$\cos(W(\psi))=\frac{r^2e^{2\psi}-1}{r^2e^{2\psi}+1}=\tanh(\psi), \tag{8}$$

where r is non-zero integral constant.

Now, we consider the conformable fractional equation of the form

$$F\left(g,\mathcal{D}_t^{\alpha}g,\mathcal{D}_y^{\alpha}g,\mathcal{D}_{tt}^{2\alpha}g,\mathcal{D}_{yy}^{2\alpha}g,\mathcal{D}_{yt}^{2\alpha}g,\ldots\right)=0. \tag{9}$$

The fractional wave transformation $\psi=\left(a\frac{y^{\alpha}}{\alpha}+v\frac{t^{\alpha}}{\alpha}\right)$ reduces Eq. (9) to the subsequent nonlinear equation.

$$\breve{F}(Q,Q',Q'',Q''',\ldots\ldots)=0. \tag{10}$$

In agreement with the SGE approach, the solution of Eq. (10) can be considered in the following form:

$$Q(\psi)=A_0+\sum_{j=1}^{N}\tanh^{j-1}(\psi)\left(B_j\operatorname{sech}(\psi)+A_j\tanh(\psi)\right), \tag{11}$$

With the assistance of (7) and (8), Eq. (11) can be rewritten as

$$Q(W)=A_0+\sum_{j=1}^{N}\cos^{j-1}(W)\left(B_j\sin(W)+A_j\cos(W)\right), \tag{12}$$

The value of the positive integer N in Eq. (12) may be calculated by applying the homogeneous balancing principle to the highest-order derivative terms and leading nonlinear terms in Eq. (10). Substituting the predicted solution (12) into (10) and taking the coefficients of like powers of $\sin(W)\cos(W)$ as zero, we get the system of algebraic equations. By solving the given system of equations, we determine the corresponding values of A_0, A_1, A_2, B_1, $B_2,\ldots,a$, and c. Then the required solutions, if they exist, are built using Eqs. (7) and (8) and ψ.

Extraction of analytical solutions

The aim of this module is to implement the SGE method to obtain expansive, consistent, and stable soliton solutions to Kudryashov's fractional generalized nonlinear refractive index model

and the Ginzburg-Landau complex fractional FCGL equation, reproducing several established solutions and introducing new explicit waveforms documented in recent studies.

4.1. The generalized form of the fractional nonlinear refractive index model

Assume the solution of Eq. (1) has the traveling wave solution of the form

$$u(x,t)=U(\xi)e^{iQ}. \tag{13}$$

The wave variables ξ and Q are defined by

$$\xi=\eta\left(\frac{x^{\alpha}}{\alpha}-v\frac{t^{\alpha}}{\alpha}\right), \text{ and } Q=-k\frac{x^{\alpha}}{\alpha}+\omega\frac{t^{\alpha}}{\alpha}+\vartheta, \tag{14}$$

where η, v, ω, k, and ϑ are the width of the soliton, wave velocity, wave frequency, wave number, and phase constant, respectively.

Using the transformation (13) and (14), the nonlinear Schrödinger Eq. (1) is separated into real and imaginary parts. The imaginary part of the equation is

$$\eta U^{2m}U'\left(\lambda+\alpha+2m(\theta+\lambda)\right)+U'\eta\left(v+2ak\right)=0. \tag{15}$$

Eq. (15) gives

$$\lambda+\alpha+2m(\theta+\lambda)=0, \text{ and } v=-2ak. \tag{16}$$

The real part of the equation is

$$\begin{aligned} &a\eta^2U''-U\left(\omega+ak^2\right)+b_1U^{1-4n}+b_2U^{1-3n}+b_3U^{1-2n}+b_4U^{1-n}\\ &+b_5U^{1+n}+b_6U^{1+2n}+b_7U^{1+3n}+b_8U^{1+4n}-k(\lambda+\mu)U^{2m+1}=0. \end{aligned} \tag{17}$$

We assume the transformation

$$U(\xi)=\varphi^{\frac{1}{2n}}. \tag{18}$$

By using Eq. (18) and considering $b_2=b_4=b_5=b_7=0$, Eq. (17) can be written as

$$\begin{aligned} &-4n^2\varphi^2\left(\omega+ak^2\right)+a\eta^2\left(2n\varphi\varphi''+(1-2n)(\varphi')^2\right)+4b_1n^2\\ &+4b_3n^2\varphi+4b_6n^2\varphi^3+4b_8n^2\varphi^4-4kn^2(\lambda+\mu)\varphi^{\frac{m}{n}+2}=0, \end{aligned} \tag{19}$$

and this leads to the solution of:

$$\begin{aligned} &iD_t^{\alpha}u+aD_x^{2\alpha}u+\left(\frac{b_1}{|u|^{4n}}+\frac{b_3}{|u|^{2n}}+b_6|u|^{2n}+b_8|u|^4\right)u\\ &=i\left(\lambda D_x^{\alpha}\left(u|u|^{2m}\right)+\theta D_x^{\alpha}\left(|u|^{2m}\right)u+\mu|u|^{2m}D_x^{\alpha}u\right). \end{aligned} \tag{20}$$

To make it solvable, let $m=2n$, then Eq. (19) can be rewritten as

$$\begin{aligned} &-4n^2\varphi^2\left(\omega+ak^2\right)+a\eta^2\left(2n\varphi\varphi''+(1-2n)(\varphi')^2\right)\\ &+4b_1n^2+4b_3n^2\varphi+4b_6n^2\varphi^3+4b_8n^2\varphi^4-4kn^2(\lambda+\mu)\varphi^4=0. \end{aligned} \tag{21}$$

The balancing principle between φ^4 and $\varphi\varphi''$ gives $4N=2N+2$, where N is the degree of the polynomial in Eq. (11), and thus we find $N=1$. Then the solution of Eq. (21) can be taken as

$$\varphi(\xi)=A_0+B_1\sin(w)+A_1\cos(w), \tag{22}$$

where A_0, A_1, and B_1 are unknown parameters to be determined. Differentiating Eq. (22) with respect to ξ, we get

$$\varphi' = B_1 \cos(w)\sin(w) - A_1 sin^2(w). \tag{23}$$

Again, differentiating Eq. (23) with respect to ξ, we have

$$\varphi'' = -B_1 sin^3(w) + B_1 cos^2(w)\sin(w) - 2A_1 sin^2(w)\cos(w), \tag{24}$$

where $\frac{dw}{d\xi} = \sin(w(\xi))$.

By substituting the Eqs. (22), (23), and (24) into Eq. (21) and then equating the coefficients of similar powers of $\sin(w)\cos(w)$, we achieved some algebraic system of equations. Using Maple to solve this algebraic system, we derived the following set of solutions:

Set 1:

$$B_1 = 0, \quad \omega = \frac{a\left(3A_0^2\eta^2 - \eta^2 A_1^2 - 2n^2k^2A_1^2\right)}{2n^2A_1^2},$$

$$b_1 = \frac{a\eta^2\left(-A_0^4 + 2A_0^2A_1^2 + 2nA_0^4 - 4nA_0^2A_1^2 - A_1^4 + 2nA_1^4\right)}{4n^2A_1^2}, \quad b_3 = -\frac{a\eta^2\, A_0\left(-A_0^2 + A_1^2 + nA_0^2 - nA_1^2\right)}{n^2A_1^2},$$

$$b_6 = \frac{a\eta^2\, A_0(1+n)}{n^2A_1^2}, \quad b_8 = -\frac{\left(a\eta^2 - 4kn^2\mu A_1^2 + 2na\eta^2 - 4kn^2\lambda A_1^2\right)}{n^2A_1^2}.$$

Set 2:

$$A_1 = 0, \quad \omega = -\frac{a\left(6A_0^2\eta^2 - \eta^2B_1^2 + 4n^2k^2B_1^2\right)}{4n^2B_1^2}, \quad b_8 = \frac{\left(a\eta^2 + 4kn^2\mu B_1^2 + 2na\eta^2 + 4kn^2\lambda B_1^2\right)}{4n^2B_1^2},$$

$$b_1 = -\frac{A_0^2a\eta^2\left(-A_0^2 - 2nB_1^2 + B_1^2 + 2nA_0^2\right)}{4n^2B_1^2}, \quad b_3 = \frac{a\eta^2\, A_0\left(B_1^2 - nB_1^2 - 2A_0^2 + 2nA_0^2\right)}{2n^2B_1^2},$$

$$b_6 = -\frac{a\eta^2\, A_0(1+n)}{n^2B_1^2}.$$

Set 3:

$$A_1 = \pm iB_1, \ \omega = -\frac{a\left(3A_0^2\eta^2 + \eta^2B_1^2 + 8n^2k^2B_1^2\right)}{8n^2B_1^2}, \ b_8 = \frac{\left(a\eta^2 + 16kn^2\mu B_1^2 + 2na\eta^2 + 16kn^2\lambda B_1^2\right)}{16n^2B_1^2},$$

$$b_1 = -\frac{a\eta^2(2n-1)\left(2A_0^2B_1^2 + B_1^4 + A_0^4\right)}{16n^2B_1^2}, \ b_3 = \frac{a\eta^2\, A_0\left(-B_1^2 + nB_1^2 - A_0^2 + nA_0^2\right)}{4n^2B_1^2}, b_6 = -\frac{a\eta^2\, A_0(1+n)}{4n^2B_1^2}.$$

Using the solutions stated earlier from the algebraic system of equations, we can construct the solution to Eq. (1) as follows:

For Set 1: Solution of Eq. (1) together with the Eqs. (11), (13), (18), and (22) can be written as

$$u(x,t) = \left(A_0 + A_1\tanh(\xi)\right)^{\frac{1}{2n}} e^{iQ}. \tag{25}$$

By the transformations

$$\xi = \eta\left(\frac{x^\alpha}{\alpha} + 2ak\frac{t^\alpha}{\alpha}\right)$$

$$\text{and } Q = -k\frac{x^\alpha}{\alpha} + \left(\frac{a\left(3A_0^2\eta^2 - \eta^2A_1^2 - 2n^2k^2A_1^2\right)}{2n^2A_1^2}\right)\frac{t^\alpha}{\alpha} + \vartheta,$$

and simplifying, solution (25) can be written as

$$u(x,t)=\left(A_0+A_1\tanh\left(\eta\left(\frac{x^\alpha}{\alpha}+2ak\frac{t^\alpha}{\alpha}\right)\right)\right)^{\frac{1}{2n}} \times\exp\left[i\left(-k\frac{x^\alpha}{\alpha}+\left(\frac{a\left(3A_0^2\eta^2-\eta^2A_1^2-2n^2k^2A_1^2\right)}{2n^2A_1^2}\right)\frac{t^\alpha}{\alpha}+\vartheta\right)\right]. \tag{26}$$

For Set 2: Solution of Eq. (1) together with Eqs. (11), (13), (18), and (22) can be written as

$$u(x,t)=\left(A_0+B_1\mathrm{sech}(\xi)\right)^{\frac{1}{2n}}e^{iQ}. \tag{27}$$

By the transformations $Q=\frac{-kx^\alpha}{\alpha}+\left(\frac{-a\left(6A_0^2\eta^2-\eta^2B_1^2+4n^2k^2B_1^2\right)}{4n^2B_1^2}\right)\frac{t^\alpha}{\alpha}+\vartheta$ and $\xi=\eta\left(\frac{x^\alpha}{\alpha}+\frac{2akt^\alpha}{\alpha}\right)$, and simplifying solution (27) can be rewritten as

$$u(x,t)=\left(A_0+B_1\mathrm{sech}\left(\eta\left(\frac{x^\alpha}{\alpha}+2ak\frac{t^\alpha}{\alpha}\right)\right)\right)^{\frac{1}{2n}} \times\exp\left[i\left(-k\frac{x^\alpha}{\alpha}-\left(\frac{a\left(6A_0^2\eta^2-\eta^2B_1^2+4n^2k^2B_1^2\right)}{4n^2B_1^2}\right)\frac{t^\alpha}{\alpha}+\vartheta\right)\right]. \tag{28}$$

For Set 3: Solution of Eq. (1) together with Eqs. (11), (13), (18), and (22) can be written as

$$u(x,t)=\left(A_0+B_1\mathrm{sech}(\xi)\pm B_1\tanh(i\xi)\right)^{\frac{1}{2n}}e^{iQ}. \tag{29}$$

By using the transformations $Q=\frac{-kx^\alpha}{\alpha}+\left(\frac{-a\left(3A_0^2\eta^2+\eta^2B_1^2+8n^2k^2B_1^2\right)}{8n^2B_1^2}\right)\frac{t^\alpha}{\alpha}+\vartheta$, and $\xi=\eta\left(\frac{x^\alpha}{\alpha}+2ak\frac{t^\alpha}{\alpha}\right)$, and simplifying, solution (28) can be rewritten as

$$u(x,t)=\left(A_0+B_1\mathrm{sech}\left(\eta\left(\frac{x^\alpha}{\alpha}+2ak\frac{t^\alpha}{\alpha}\right)\right)\pm B_1\tanh\left(\eta i\left(\frac{x^\alpha}{\alpha}+2ak\frac{t^\alpha}{\alpha}\right)\right)\right)^{\frac{1}{2n}} \times\exp\left[i\left(-k\frac{x^\alpha}{\alpha}-\left(\frac{a\left(3A_0^2\eta^2+\eta^2B_1^2+8n^2k^2B_1^2\right)}{8n^2B_1^2}\right)\frac{t^\alpha}{\alpha}+\vartheta\right)\right]. \tag{30}$$

Similarly, varying the free parameters yields a broader set of intricate solutions to Kudryashov's generalized refractive form of the fractional nonlinear Schrödinger equation. For brevity, these are not included in this analysis.

4.2. The fractional complex Ginzburg-Landau equation

We assumed the solution of Eq. (2) is of the form

$$\phi(x,t)=u(\eta)e^{iQ}. \tag{31}$$

The wave variables η and Q are defined as

$$\eta=\left(\frac{x^\alpha}{\alpha}-v\frac{t^\alpha}{\alpha}\right)$$
and
$$Q=-k\frac{x^\alpha}{\alpha}+\omega\frac{t^\alpha}{\alpha}+\vartheta, \tag{32}$$

Inserting Eqs. (31) and (32) into Eq. (2), and simplifying, we get

$$\left(-\omega u + a\left(u'' - uk^2\right) + bH\left(u^2\right)u - 2\left(\nu - 2\beta\right)\frac{u'^2}{u} - 2\nu\, u'' - \delta u\right)e^{iQ} + i\left(-\nu u' - 2aku'\right)e^{iQ} = 0. \tag{33}$$

Since $e^{iQ} \neq 0$, the above equation becomes

$$-\omega u + a\left(u'' - uk^2\right) + bH\left(u^2\right)u - 2\left(\nu - 2\beta\right)\frac{u'^2}{u} - 2\nu u'' - \delta u - i\left(\nu u' + 2aku'\right) = 0. \tag{34}$$

Now, we separate the imaginary and real parts of Eq. (34). The imaginary part of Eq. (34) is

$$\nu u' + 2aku' = 0. \tag{35}$$

Since $u' \neq 0$, thus, from Eq. (35), we obtain

$$\nu = -2ak. \tag{36}$$

Eq. (36) gives the velocity of the soliton.
The real part of Eq. (34) is

$$-\omega u + a\left(u'' - uk^2\right) + bH\left(u^2\right)u - 2\left(\nu - 2\beta\right)\frac{u'^2}{u} - 2\nu\, u'' - \delta u = 0. \tag{37}$$

To remove the singularity, we assume $\nu = 2\beta$. From a physical point of view, a singular equation means the model ceases to work or changes its behavior when the variable u becomes zero. Such equations are studied in nonlinear wave theory since they can describe real phenomena, such as sharp-peaked solitary waves, compactons, peakons, and wave breaking that a smoother, regular model cannot describe. Then the above equation takes the following form

$$\left(a - 4\beta\right)u'' - \left(\omega + ak^2 + \delta\right)u + bH\left(u^2\right)u = 0. \tag{38}$$

Power-law nonlinearity can be considered a generalization of the Kerr power-law nonlinearity. In this case, the function $H(u)$ is defined as $H(u) = u^n$. Therefore, Eq. (38) can be rewritten as

$$\left(a - 4\beta\right)u'' - \left(\omega + ak^2 + \delta\right)u + bu^{2n+1} = 0. \tag{39}$$

Here, in Eq. (39), the parameter n indicates the power-law nonlinearity. The condition $0<n<2$, and in particular $n\neq 2$, ensures that the model describes stable and physically meaningful wave propagation, whereas values outside this range may correspond to unstable or nonphysical behavior. Since the balance principle fails in Eq. (39), we consider the transformation

$$u = U^{\frac{1}{2n}}. \tag{40}$$

Using the above transformation into Eq. (39) and simplifying, we obtain

$$\left(a - 4\beta\right)\left(\left(1 - 2n\right)U'^2 + 2nUU''\right) - 4n^2\left(\omega + ak^2 + \delta\right)U^2 + 4bn^2U^3 = 0. \tag{41}$$

The balancing norm between U^3 and UU'' yields $3N = 2N + 2$, and we find $N = 2$. Now, the solution of Eq. (41) can be taken as

$$U(\eta) = a_0 + b_1\sin(w) + a_1\cos(w) + b_2\sin(w)\cos(w) + a_2\cos^2(w). \tag{42}$$

Here, a_0, a_1, a_2, b_1, and b_2 are undefined constants that are not specified in advance. Their values are determined systematically during the solution process by substituting them into the governing equations and applying the necessary constraints. Differentiating Eq. (42) with respect to η, we attain

$$U' = b_1\cos(w)\sin(w) - a_1\sin^2(w) + b_2\cos^2(w)\sin(w) - b_2 sin^3(w) - 2a_2\cos(w) sin^2(w). \tag{43}$$

Again, differentiating Eq. (43) with respect to η, it becomes

$$U'' = -b_1\sin^3(w) + b_1\cos^2(w)\sin(w) - 2a_1\sin^2(w)\cos(w) - 5b_2\cos(w)\sin^3(w) + b_2\cos^3(w)\sin(w) + 2a_2\sin^4(w) - 4a_2\cos^2(w)\sin^2(w), \tag{44}$$

with $\frac{dw}{d\eta} = \sin(w(\eta))$.

By substituting Eqs. (42)-(44) into Eq. (41) and equating the coefficients of similar powers of $\sin(w)\cos(w)$, we can simplify Eq. (41) into an algebraic system of equations. Using Maple to solve this algebraic system, we derived the following set of solutions:

Set 1:

$$\omega = -\frac{n^2ak^2 + n^2\delta + 4\beta - a}{n^2},\ a_1 = b_1 = b_2 = 0,\ a_0 = \frac{a - 4\beta + an - 4\beta n}{bn^2},$$

$$a_2 = -\frac{a - 4\beta + an - 4\beta n}{bn^2}.$$

Set 2:

$$\omega = -\frac{4n^2ak^2 + 4n^2\delta + 4\beta - a}{4n^2},\ a_0 = \frac{a - 4\beta + an - 4\beta n}{2bn^2},\ a_1 = 0,\ b_1 = 0,$$

$$a_2 = -\frac{a - 4\beta + an - 4\beta n}{2bn^2},\ b_2 = \frac{\pm i(a - 4\beta)(1 + n)}{2bn^2}.$$

By utilizing the solutions established previously, Eq. (2) can be resolved accordingly:

For Set 1: The solution of Eq. (41) with Eq. (11) can be written as

$$U(\eta) = \left(\frac{a - 4\beta + an - 4\beta n}{bn^2}\right) - \left(\frac{a - 4\beta + an - 4\beta n}{bn^2}\right)\tanh^2(\eta). \tag{45}$$

Therefore, Eq. (40) becomes

$$u(\eta) = \left[\left(\frac{a - 4\beta + an - 4\beta n}{bn^2}\right) - \left(\frac{a - 4\beta + an - 4\beta n}{bn^2}\right)\tanh^2(\eta)\right]^{\frac{1}{2n}}. \tag{46}$$

The wave variables η and Q with Eq. (36) can be written as

$$\eta = \left(\frac{x^\alpha}{\alpha} + 2ak\frac{t^\alpha}{\alpha}\right), \text{and } Q = -k\frac{x^\alpha}{\alpha} - \left(\frac{n^2ak^2 + n^2\delta + 4\beta - a}{n^2}\right)\frac{t^\alpha}{\alpha} + \vartheta.$$

Hence, the solution of Eq. (2), together with Eq. (31), is achieved as follows

$$\phi(x,t) = \left[\left(\frac{a - 4\beta + an - 4\beta n}{bn^2}\right) - \left(\frac{a - 4\beta + an - 4\beta n}{bn^2}\right)\tanh^2\left(\frac{x^\alpha}{\alpha} + 2ak\frac{t^\alpha}{\alpha}\right)\right]^{\frac{1}{2n}} \times\exp\left[i\left(-k\frac{x^\alpha}{\alpha} - \left(\frac{n^2ak^2 + n^2\delta + 4\beta - a}{n^2}\right)\frac{t^\alpha}{\alpha} + \vartheta\right)\right]. \tag{47}$$

For Set 2: The solution of Eq. (41) with Eq. (11) can be written as

$$U(\eta) = \left(\frac{a - 4\beta + an - 4\beta n}{2bn^2}\right) + \left(\frac{\pm i(a - 4\beta)(1 + n)}{2bn^2}\right)\tanh(\eta)\operatorname{sech}(\eta) - \left(\frac{a - 4\beta + an - 4\beta n}{2bn^2}\right)\tanh^2(\eta).$$

Thus, Eq. (40) becomes

$$u(\eta)=\left[\begin{array}{l}\left(\frac{a-4\beta+an-4\beta n}{2bn^2}\right)+\left(\frac{\pm(a-4\beta)(1+n)}{2bn^2}\right)\tanh(\eta)\operatorname{sech}(\eta)\\ -\left(\frac{a-4\beta+an-4\beta n}{2bn^2}\right)\tanh^2(\eta)\end{array}\right]^{\frac{1}{2n}}.$$

The wave variables η and Q with Eq. (36) can be written as

$$\eta=\left(\frac{x^\alpha}{\alpha}+2ak\frac{t^\alpha}{\alpha}\right),$$

$$\text{and } Q=-k\frac{x^\alpha}{\alpha}-\left(\frac{4n^2ak^2+4n^2\delta+4\beta-a}{4n^2}\right)\frac{t^\alpha}{\alpha}+\vartheta.$$

Hence, the solution of Eq. (2), together with Eq. (31) achieved

$$\phi(x,t)=\left(\begin{array}{l}\left(\frac{a-4\beta+an-4\beta n}{2bn^2}\right)\pm\left(\frac{(a-4\beta)(1+n)}{2bn^2}\right)\\ \times\tanh\left(\frac{x^\alpha}{\alpha}+2ak\frac{t^\alpha}{\alpha}\right)\operatorname{sech}\left(\frac{x^\alpha}{\alpha}+2ak\frac{t^\alpha}{\alpha}\right)\\ -\left(\frac{a-4\beta+an-4\beta n}{2bn^2}\right)\tanh^2\left(\frac{x^\alpha}{\alpha}+2ak\frac{t^\alpha}{\alpha}\right)\end{array}\right)^{1/2n}\times\exp\left[i\left(-k\frac{x^\alpha}{\alpha}-\left(\frac{4n^2ak^2+4n^2\delta+4\beta-a}{4n^2}\right)\frac{t^\alpha}{\alpha}+\vartheta\right)\right]. \quad (48)$$

Similarly, varying the free parameters yields a broader set of intricate solutions to the fractional complex Ginzburg-Landau equation. For the sake of brevity, these are not included in this analysis.

Results and discussion

In this section, we will discuss the results obtained through graphical representations of the solutions for different parameter values. We draw the graph of these solutions by using the symbolic computation tool Mathematica.

5.1. The generalized form of the fractional nonlinear refractive index model

In this section, we describe the graphical representation of the obtained solutions of Kudryashov's generalized form of the fractional nonlinear refractive index model for different values of the parameters. The 3-dimensional plot, 2-dimensional plot, density plot, and contour plot of the accomplished solutions are provided below:

The absolute value of solution (26) gives the kink-shaped soliton for the definite values $A_0=A_1=10$, $a=0.5$, $k=-0.4$, $n=0.3$, $\eta=-3$, $\vartheta=2$, and $\alpha=0.9$. Fig. 1a 3D and Fig. 1c contour graphs are drawn within the interval $0\le x$, $t\le 10$. For $t=6$, the 2D plot is represented in Fig. 1b with the same interval. If we increase the value of η from -3 to 2.5 while the remaining parameters are the same, the absolute value of the solution (26) represents the anti-kink wave type soliton with the interval $0\le x\le 10$, $0\le t\le 10$. Fig. 2a 3D plot, Fig. 2b 2D plot for $t=6$, and Fig. 2c contour plot are illustrated. Breather soliton is obtained from the real part of Eq. (26) for the corresponding value of $A_0=30$, $A_1=10$, $a=1$, $k=2.6$, $n=0.44$, $\eta=-5.2$, $\vartheta=4$, and $\alpha=0.99$ with the interval $0\le x$, $t\le 20$. Fig. 3a 3D plot, Fig. 3b 2D plot at $t=15$, and Fig.3c density plot are presented. For definite values of

$A_0 = 7.6$, $A_1 = 10$, $a = 0.22$, $k = 7$, $n = 0.33$, $\eta = 0.5$, $\vartheta = 4$, and $\alpha = 0.99$, the real part of Eq. (26) represents the periodic soliton, which is shown in Fig. 4a 3D plot, Fig. 4b 2D plot for $t = 1.5$, and Fig. 4c contour plot with the interval $0 \le x$, $t \le 2$. The imaginary part of Eq. (26) gives the periodic soliton, which is traveling along the t-direction for a certain value of $A_0 = 4$, $A_1 = 25$, $a = 1$, $k = 7$, $n = 0.33$, $\eta = 2$, $\vartheta = 7$, and $\alpha = 0.99$ with the interval $0 \le x \le 20$, $0 \le t \le 2$. 3D and contour graphs are represented in Fig. 5a and Fig. 5c. Further, the 2D plot for $x = 10$, is shown in Fig. 5b.

The modulus of Eq. (28) represents the W-shape wave soliton for definite values of the parameters $a = 0.2$, $k = -2.6$, $n = 0.3$, $\alpha = 0.9$, $\vartheta = 2.2$, $A_0 = 10$, $B_1 = -21$, and $\eta = 1.5$. Fig. 6a 3D, Fig. 6b 2D plot for $t = 5$, and Fig. 6c contour graphs are depicted within the interval $0 \le x$, $t \le 10$. Keeping all the parameters constant without B_1, the modulus of Eq. (28) gives the anti-bell-shaped soliton for $B_1 = -7$ and the bell-shaped soliton for $B_1 = 7$ with the same interval. The 3D plots, (2D for $t = 5$), and contour plots are shown in Fig. 7 and Fig. 8.

For all values of $a = 0.2$, $k = -2.6$, $n = 0.3$, $\alpha = 0.9$, $\vartheta = 2.2$, $A_0 = 10$, $B_1 = 7$, and $\eta = -0.25$, the absolute value of Eq. (28) represents the parabolic soliton. The 3D, contour, and 2D plots for $t = 5$ are shown in Figs. 9a, 9c, and 9b within the interval $0 \le x$, $t \le 10$. If we change the value of B_1 from 7 to -7 and η from -0.25 to -5.2 while the remaining values are constant, the cusp-like dark soliton is obtained for the modulus of Eq. (28). Fig. 10a 3D plot, Fig. 10b 2D plot for $t = 5$, and Fig. 10c contour plot are illustrated in the same interval.

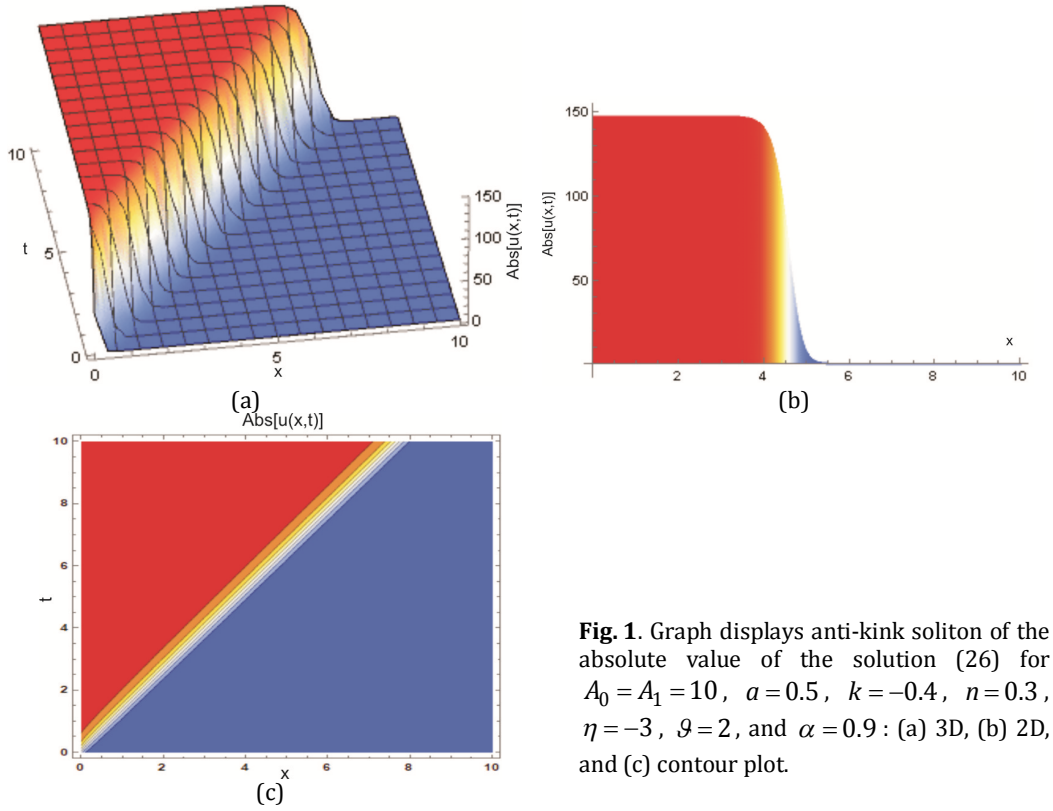

Fig. 1. Graph displays anti-kink soliton of the absolute value of the solution (26) for $A_0 = A_1 = 10$, $a = 0.5$, $k = -0.4$, $n = 0.3$, $\eta = -3$, $\vartheta = 2$, and $\alpha = 0.9$: (a) 3D, (b) 2D, and (c) contour plot.

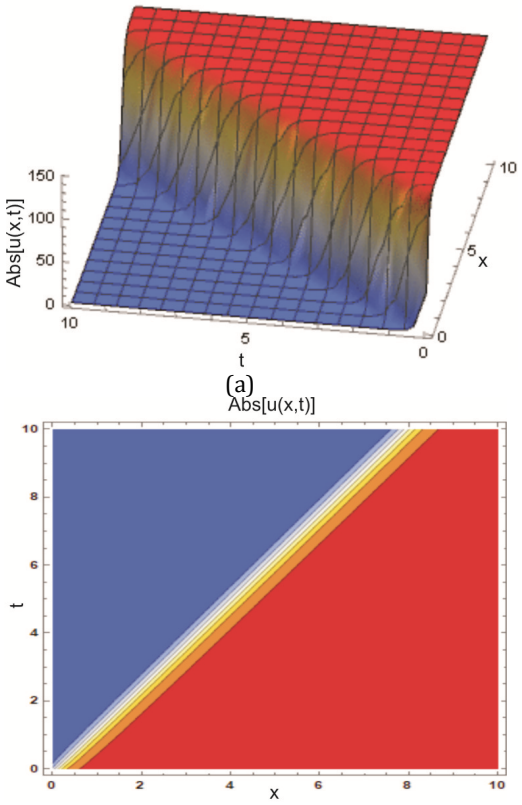

Fig. 2. Graph displays kink soliton of the absolute of the solution (26) for $A_0 = A_1 = 10$, $a = 0.5$, $k = -0.4$, $n = 0.3$, $\eta = -2.5$, $\vartheta = 2$, and $\alpha = 0.9$: (a) 3D, (b) 2D, and (c) contour plot.

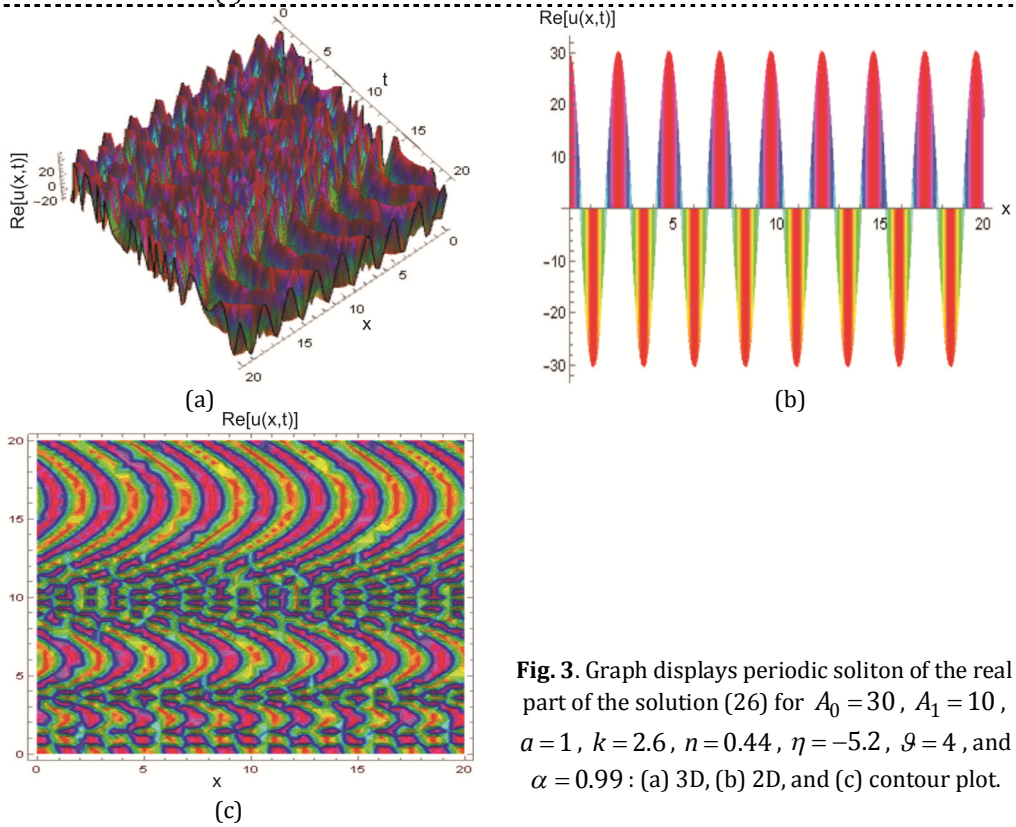

Fig. 3. Graph displays periodic soliton of the real part of the solution (26) for $A_0 = 30$, $A_1 = 10$, $a = 1$, $k = 2.6$, $n = 0.44$, $\eta = -5.2$, $\vartheta = 4$, and $\alpha = 0.99$: (a) 3D, (b) 2D, and (c) contour plot.

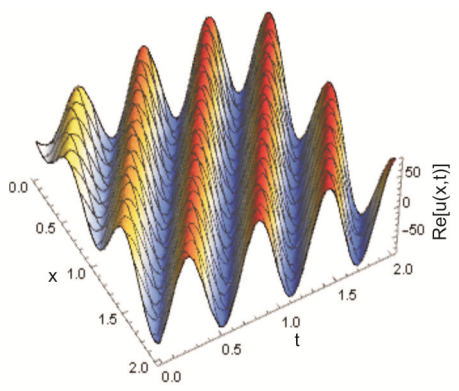

(a)

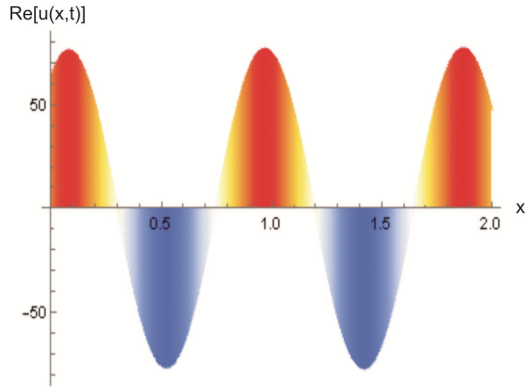

(b)

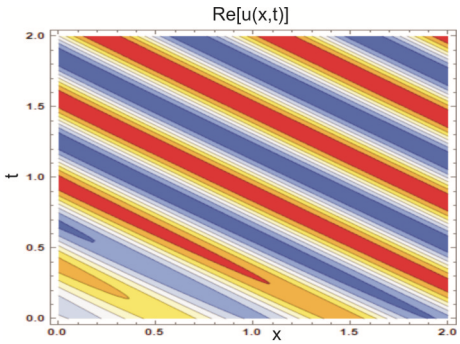

(c)

Fig. 4. Graph displays periodic soliton of the real part of the solution (26) for $A_0 = 7.6$, $A_1 = 10$, $a = 0.22$, $k = 7$, $n = 0.33$, $\eta = 0.5$, $\vartheta = 4$, and $\alpha = 0.99$: (a) 3D, (b) 2D, and (c) contour plot.

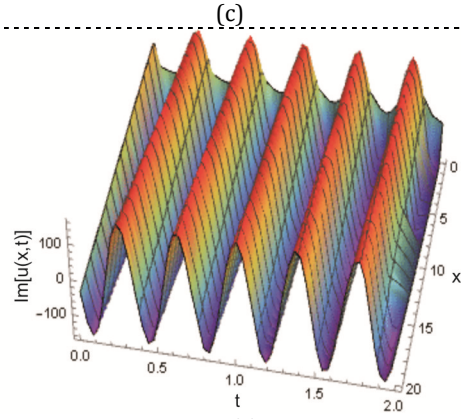

(a)

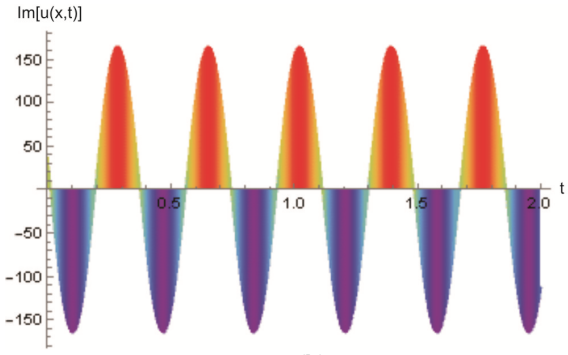

(b)

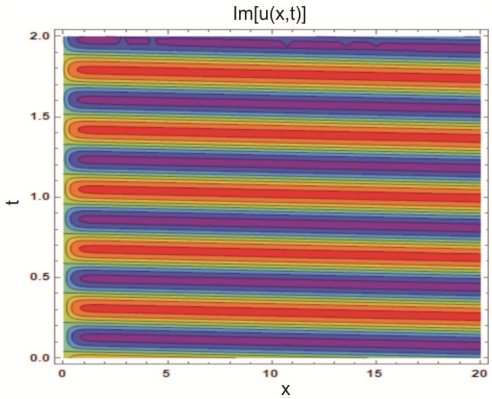

(c)

Fig. 5. Graph displays periodic soliton of the imaginary part of the solution (26) for $A_0 = 4$, $A_1 = 25$, $a = 1$, $k = 7$, $n = 0.33$, $\eta = 2$, $\vartheta = 7$, and $\alpha = 0.99$: (a) 3D, (b) 2D, and (c) contour plot.

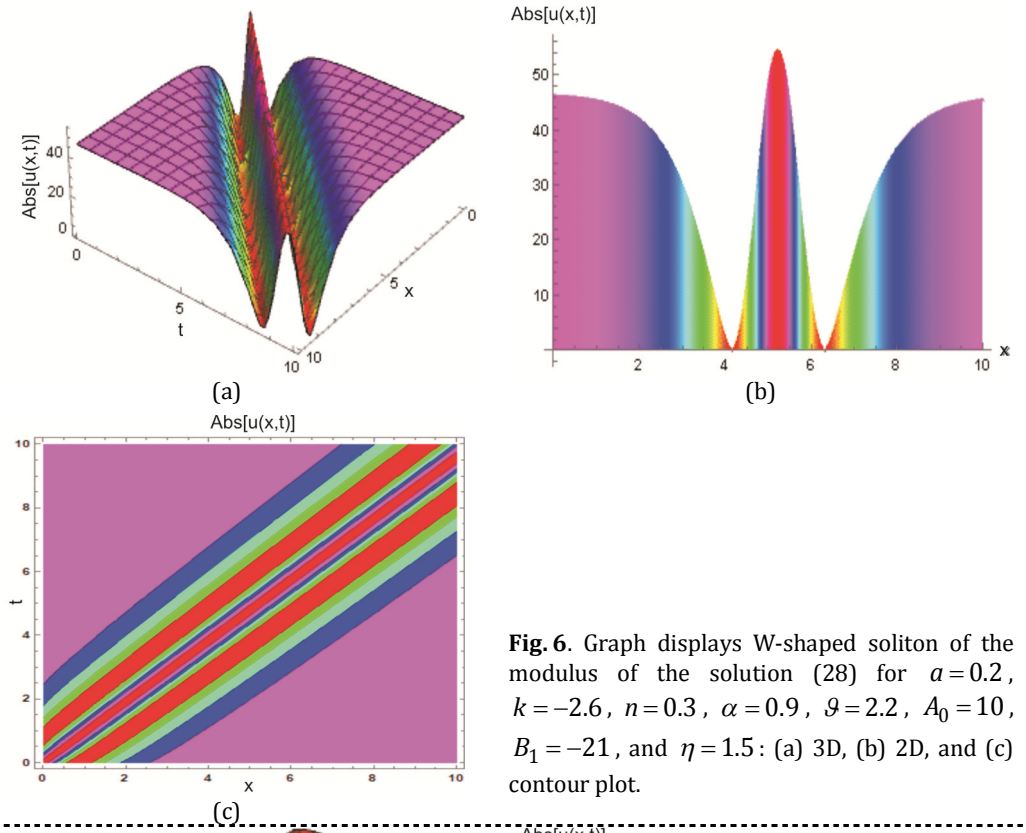

Fig. 6. Graph displays W-shaped soliton of the modulus of the solution (28) for $a=0.2$, $k=-2.6$, $n=0.3$, $\alpha=0.9$, $\vartheta=2.2$, $A_0=10$, $B_1=-21$, and $\eta=1.5$: (a) 3D, (b) 2D, and (c) contour plot.

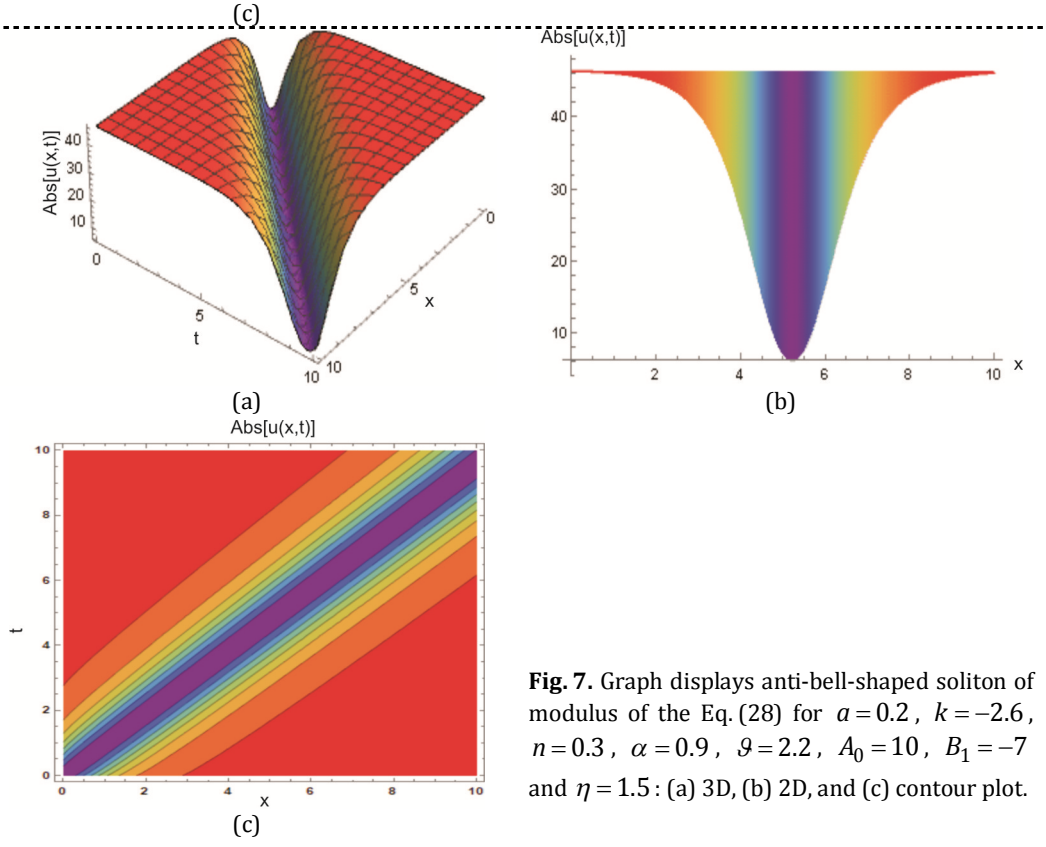

Fig. 7. Graph displays anti-bell-shaped soliton of modulus of the Eq. (28) for $a=0.2$, $k=-2.6$, $n=0.3$, $\alpha=0.9$, $\vartheta=2.2$, $A_0=10$, $B_1=-7$ and $\eta=1.5$: (a) 3D, (b) 2D, and (c) contour plot.

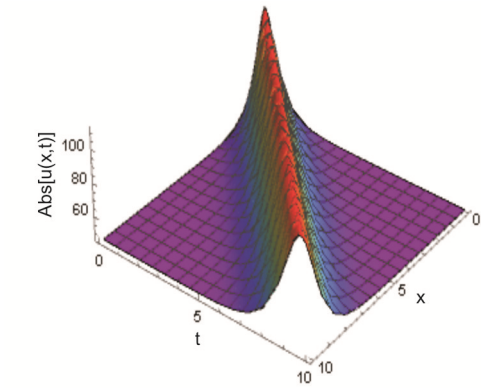

(a)

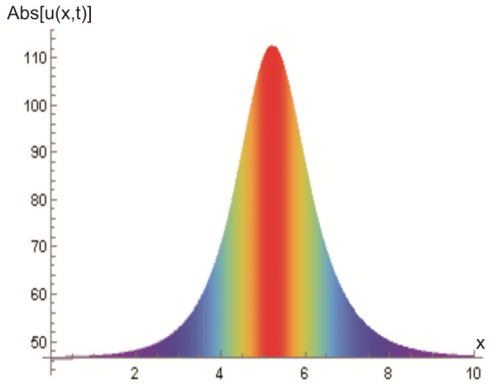

(b)

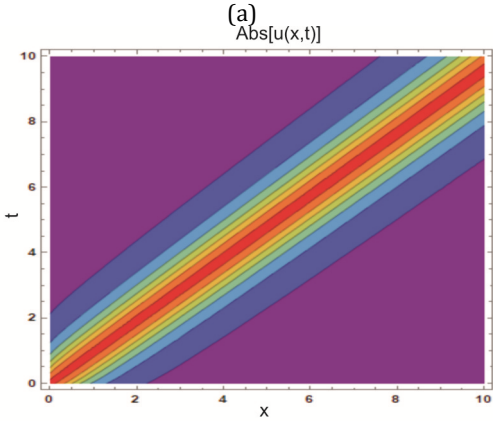

(c)

Fig. 8. Graph displays bell-shaped soliton of modulus of the equation (28) for $a=0.2$, $k=-2.6$, $n=0.3$, $\alpha=0.9$, $\vartheta=2.2$, $A_0=10$, $B_1=7$ and $\eta=1.5$: (a) 3D, (b) 2D, and (c) contour plot.

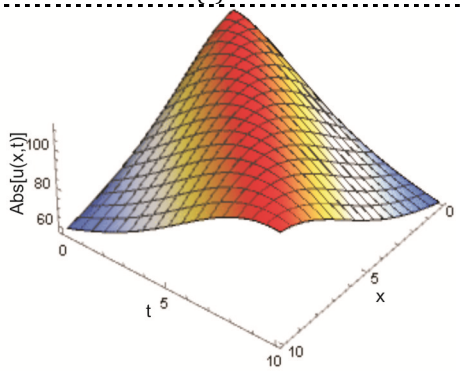

(a)

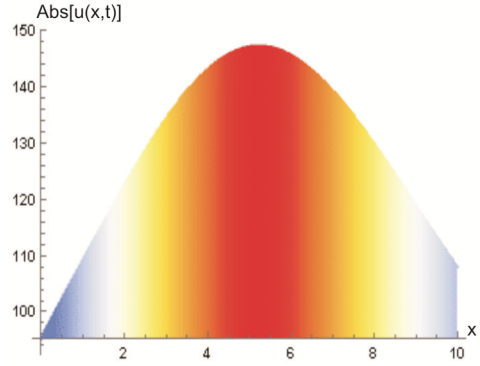

(b)

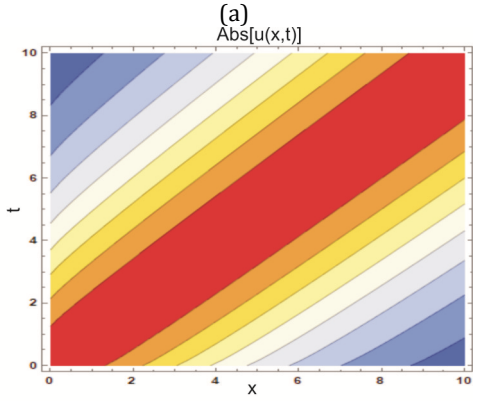

(c)

Fig. 9. Graph displays compacton of modulus of the Eq. (28) for $a=0.2$, $k=-2.6$, $n=0.3$, $\alpha=0.9$, $\vartheta=2.2$, $A_0=10$, $B_1=7$ and $\eta=-0.25$: (a) 3D, (b) 2D, and (c) contour plot.

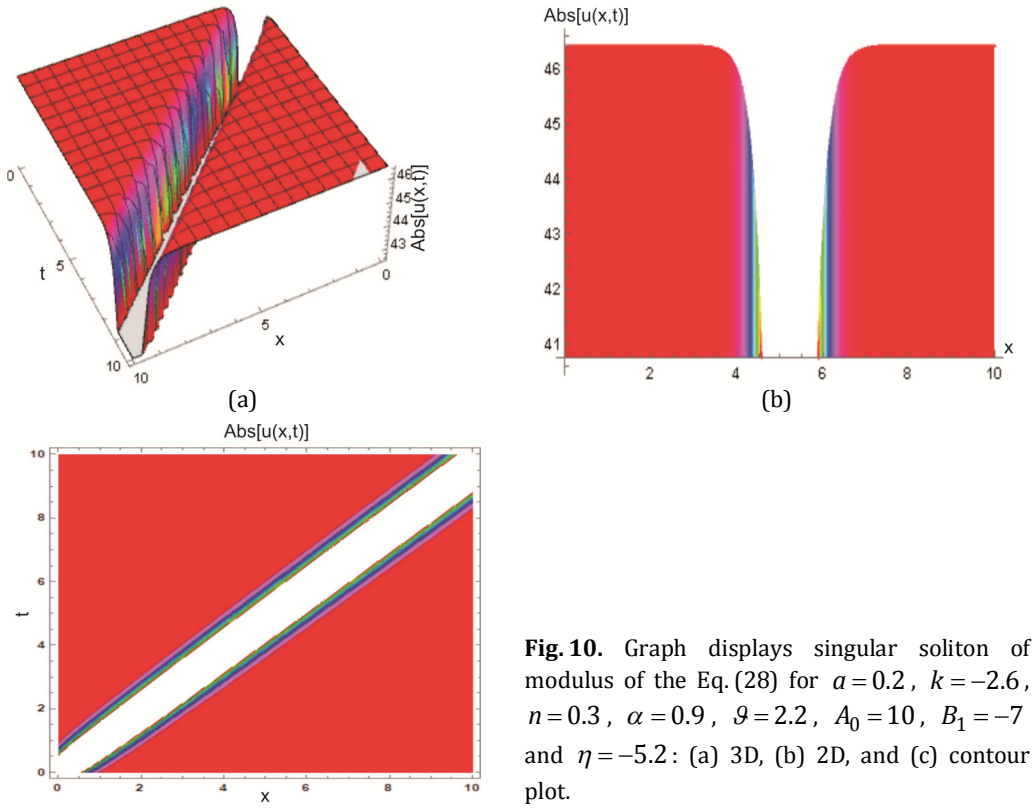

Fig. 10. Graph displays singular soliton of modulus of the Eq. (28) for $a=0.2$, $k=-2.6$, $n=0.3$, $\alpha=0.9$, $\vartheta=2.2$, $A_0=10$, $B_1=-7$ and $\eta=-5.2$: (a) 3D, (b) 2D, and (c) contour plot.

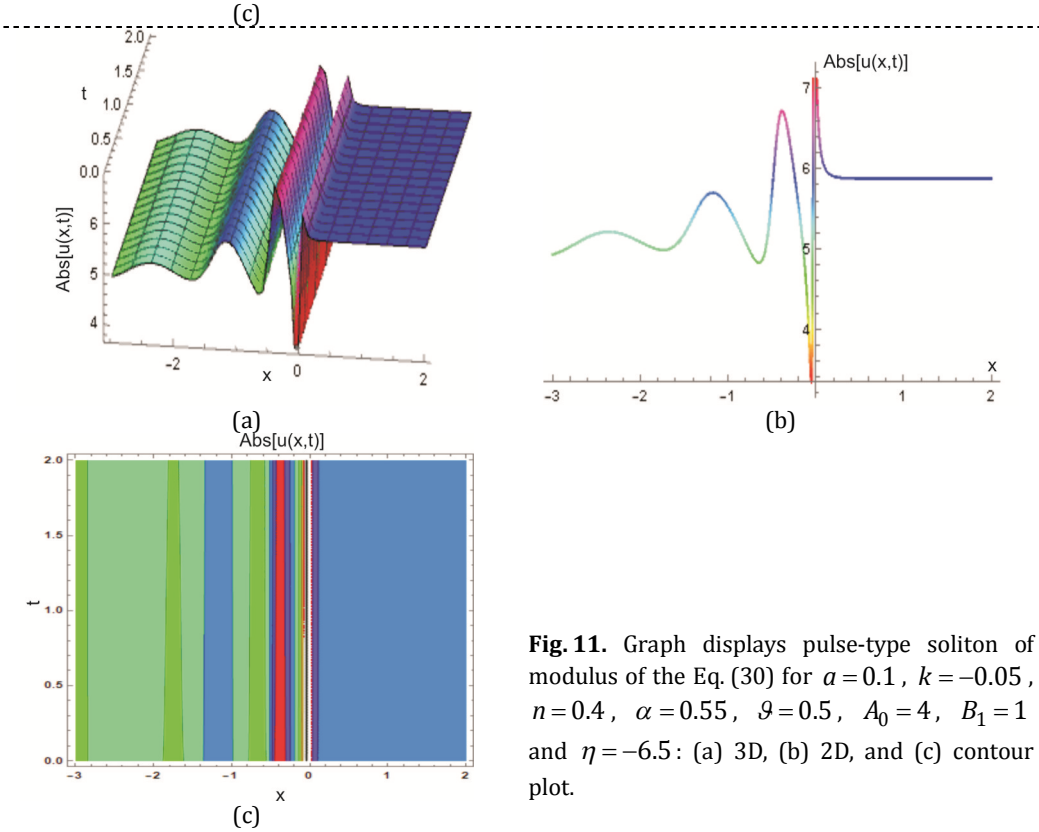

Fig. 11. Graph displays pulse-type soliton of modulus of the Eq. (30) for $a=0.1$, $k=-0.05$, $n=0.4$, $\alpha=0.55$, $\vartheta=0.5$, $A_0=4$, $B_1=1$ and $\eta=-6.5$: (a) 3D, (b) 2D, and (c) contour plot.

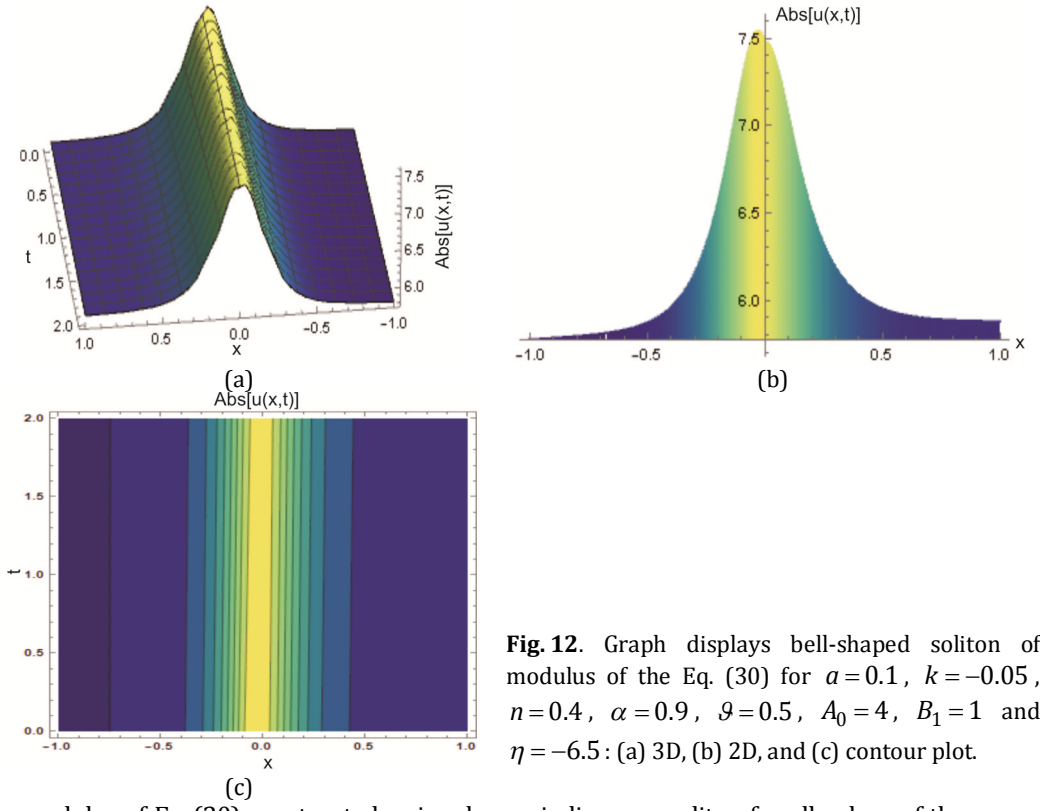

Fig. 12. Graph displays bell-shaped soliton of modulus of the Eq. (30) for $a=0.1$, $k=-0.05$, $n=0.4$, $\alpha=0.9$, $\vartheta=0.5$, $A_0=4$, $B_1=1$ and $\eta=-6.5$: (a) 3D, (b) 2D, and (c) contour plot.

The modulus of Eq. (30) constructed a singular-periodic wave soliton for all values of the parameter $a=0.1$, $k=-0.05$, $n=0.4$, $\alpha=0.55$, $\vartheta=0.5$, $A_0=4$, $B_1=1$, and $\eta=-6.5$. 3D and contour plots are drawn in the intervals $-3\le x\le 2$, $0\le t\le 2$ as shown in Fig. 1a,c. Further, for t=1.5, the 2D plot is portrayed in Fig. 11b. If we increase only the value of fractional order α from 0.55 to 0.9 while the other parameters remain the same, then the bell-shaped soliton is found modulus of the solution (30) within the intervals $-1\le x\le 1$, $0\le t\le 2$. Fig. 12a 3D graph, Fig. 12c contour graph, and Fig. 12b 2D plot for $t=1$ are drawn for the interval $-1\le x\le 1$.

From the aforementioned description of the soliton profile, we see that the soliton shape changes mostly as a result of the values of power nonlinearity n, wavenumber k, fractional order α, η, and B_1.

5.2. The space-time fractional CGL equation with power law nonlinearity

The modulus of the Eq. (47) represents the singular bright soliton for different values of a=1, b=2, k=0.06, n=0.7, $\beta=-0.09$, $\delta=0.5$, $\vartheta=1$, and $\alpha=0.99$. Fig. 13a, the 3D plot, and Fig. 13c, the contour graph are shown over the intervals $-10\le x\le 10$ and $-6\le t\le 6$. For $t=0$, the 2D graph is presented in Fig. 13b. If we increase the value of power-law nonlinearity n from 0.7 to 1.5 while the others are constant, then the modulus of the solution (47) gives the bell-shaped soliton with the same intervals. Fig. 14a 3D plot and Fig. 14b 2D plot for $t=0$ are drawn in the interval $-10\le x\le 10$, and the contour plot is shown in Fig. 14c. The real part of Eq. (47) yields a periodic-like wave soliton for the specific values a=–5, b=2, k=0.1, n=0.55, $\delta=1$, $\beta=-2$, $\vartheta=4$, and $\alpha=0.9$. Fig. 15a 3D graph and Fig. 15(c) contour graphs are represented for the interval $0\le x\le 4$, $0\le t\le 4$. Also, for $x=2$, the 2D graph is drawn in the interval $0\le t\le 4$, which is shown in Fig. 15b.

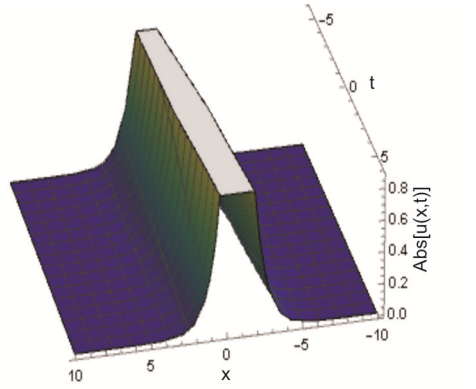

(a)

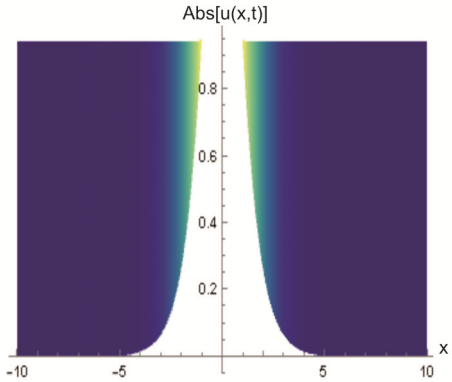

(b)

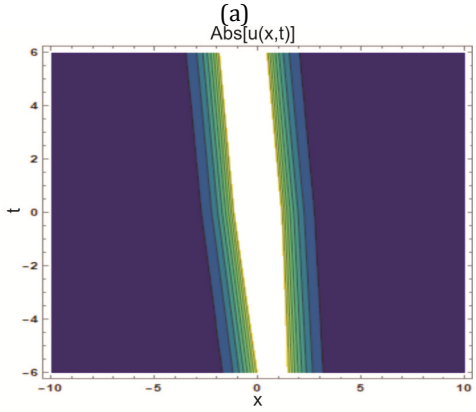

(c)

Fig. 13 Graph displays singular bright soliton of the modulus of the solution (47) for $a=1$, $b=2$, $k=0.06$, $n=0.7$, $\beta=-0.09$, $\delta=0.5$, $\vartheta=1$ and $v=0.99$: (a) 3D, (b) 2D, and (c) contour plot.

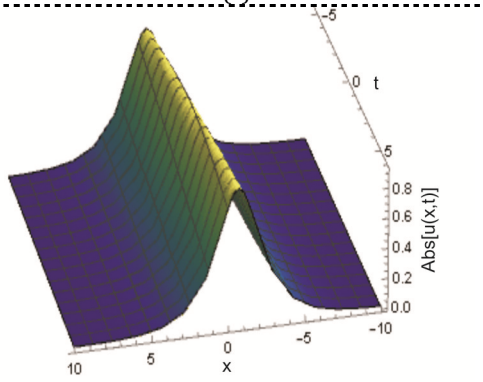

(a)

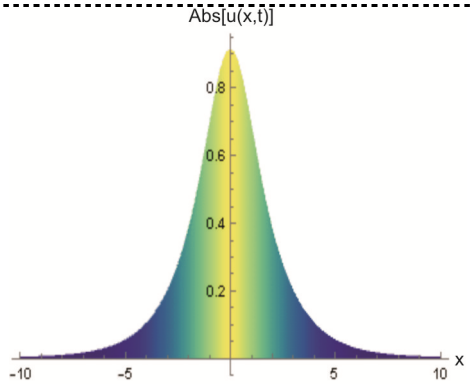

(b)

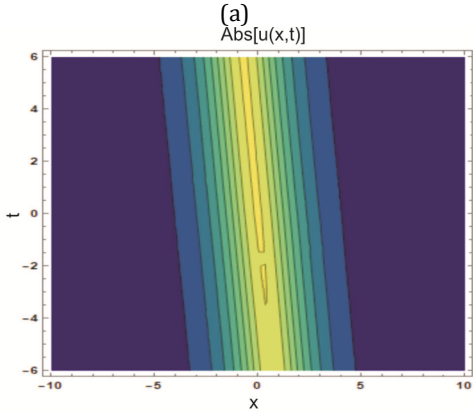

(c)

Fig. 14. Graph displays bell-shaped soliton of the modulus of the solution (47) for $a=1$, $b=2$, $k=0.06$, $n=1.5$, $\beta=-0.09$, $\delta=0.5$, $\vartheta=1$ and $v=0.99$: (a) 3D, (b) 2D, and (c) contour plot.

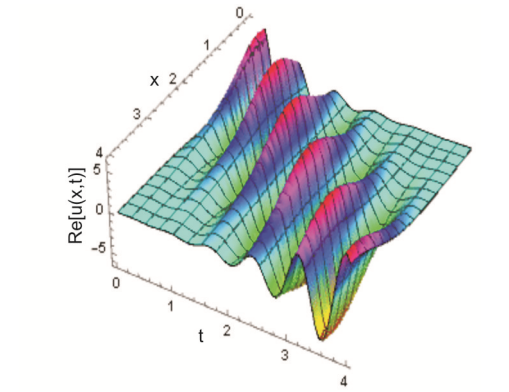

(a)

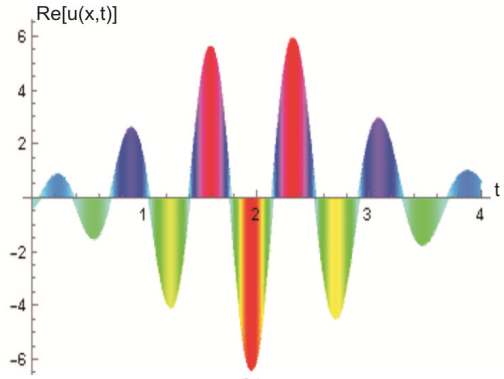

(b)

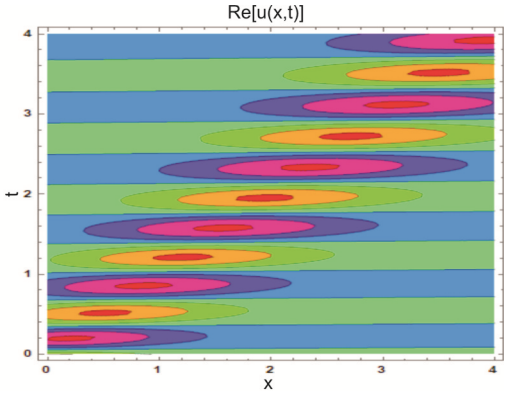

(c)

Fig. 15: Graph displays periodic soliton of the real portion of the solution (47) for $a=-5$, $b=2$, $k=0.1$, $n=0.55$, $\delta=1$, $\beta=-2$, $\vartheta=4$ and $\nu=0.9$: (a) 3D, (b) 2D, and (c) contour plot.

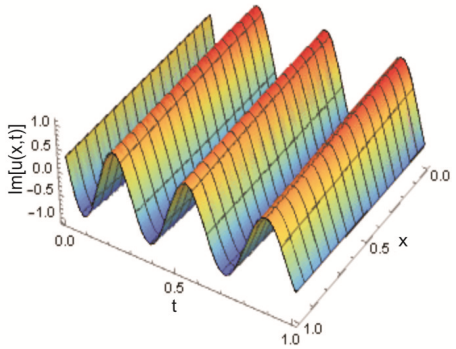

(a)

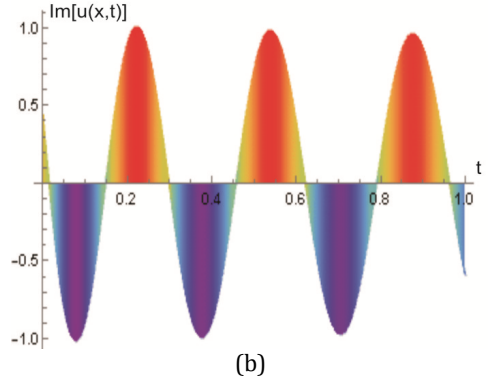

(b)

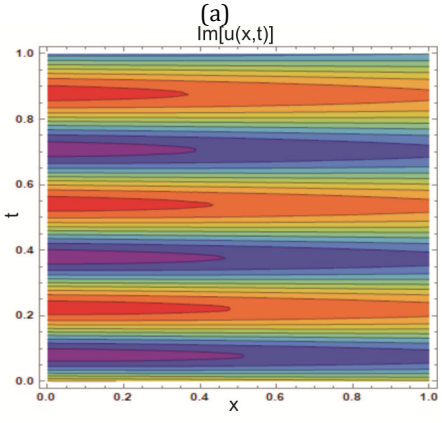

(c)

Fig. 16. Graph displays periodic soliton of the imaginary portion of the solution (47) for $a=1$, $b=-40$, $k=0.1$, $n=1.99$, $\delta=-2$, $\beta=20$, $\vartheta=0.5$ and $\nu=0.9$: (a) 3D, (b) 2D, and (c) contour plot.

The imaginary portion of the solution (47) represents the periodic soliton, which is traveling along the t-direction for a certain value of $a=1$, $b=-40$, $k=0.1$, $n=1.99$, $\delta=-2$, $\beta=20$, $\vartheta=0.5$, and $\alpha=0.9$ within the intervals $0\le x\le 1$, $0\le t\le 1$.

3D and contour graphs are presented in Fig. 16a and 1(c. Further, the 2D plot for $x=0.5$ is shown in Fig. 16b. Keeping all the values constant without β, a parabolic soliton is obtained for $\beta=0.3$ of the imaginary part of Eq. (47) in the same interval. The 3D plot, 2D plot for $x=0.5$, and contour plots are depicted over the interval $0\le x,t\le 1$ as shown in Fig. 17.

A flat-kink soliton wave is found for the modulus of the Eq. (48) for the value of $a=2.9$, $b=2.5$, $k=0.9$, $n=1.9$, $\delta=-2$, $\beta=6$, $\vartheta=1$, and $v=0.24$ within the intervals $-10\le x,t\le 0$. A 3D plot, a 2D graph for $t=-9$, and contour plots are illustrated in Fig. 18.

The absolute value of the solution (48) represents the bell-shaped soliton for the value of the parameters $a=3$, $b=2.5$, $k=0.1$, $n=1.9$, $\delta=-2$, $\beta=6$, $\theta=1$, and $v=0.99$ within the intervals $-10\le x\le 10$ and $-6\le t\le 6$. The 3D and contour graphs are shown in Fig. 19a,c.

Further, Fig. 19b represented the 2D graph for t=0. When we increase the value of wave number k from 0.1 to 1.8 while the other variables are constant, then a singular bright soliton is formed in the same intervals. 3D plot, a 2D plot for x=0, and contour graphs are presented in Fig. 20.

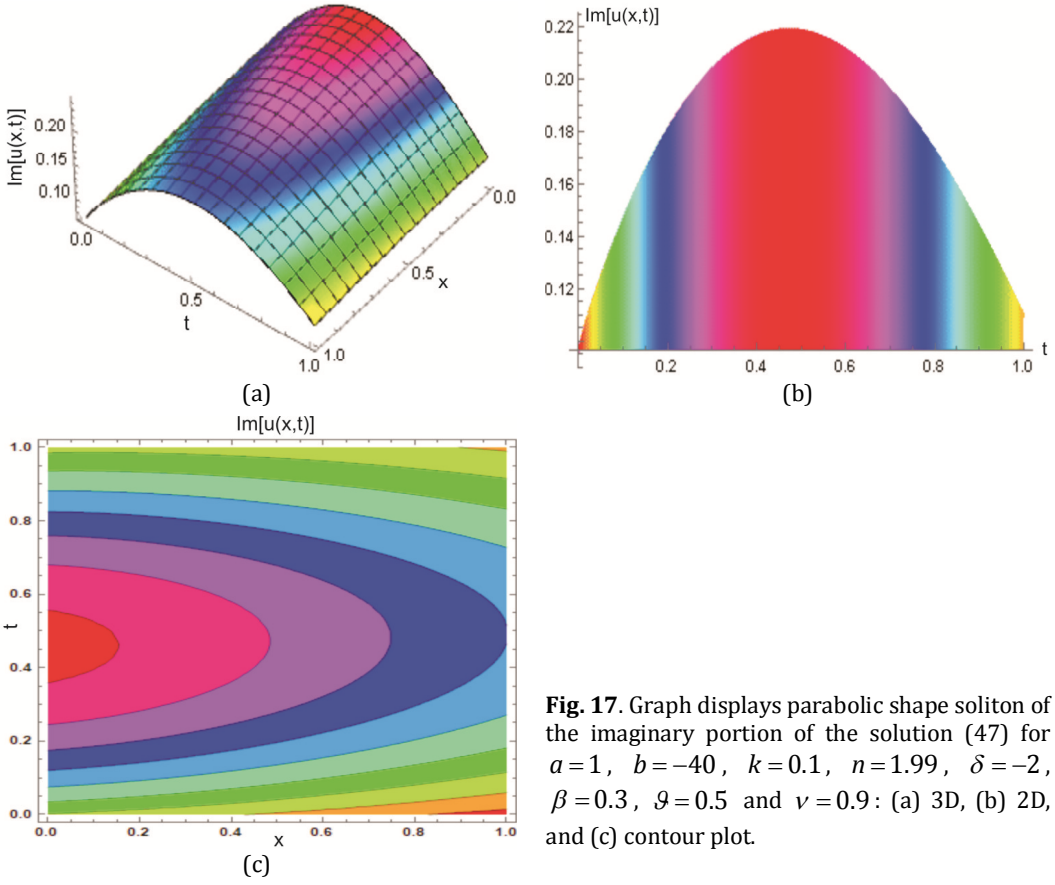

Fig. 17. Graph displays parabolic shape soliton of the imaginary portion of the solution (47) for $a=1$, $b=-40$, $k=0.1$, $n=1.99$, $\delta=-2$, $\beta=0.3$, $\vartheta=0.5$ and $v=0.9$: (a) 3D, (b) 2D, and (c) contour plot.

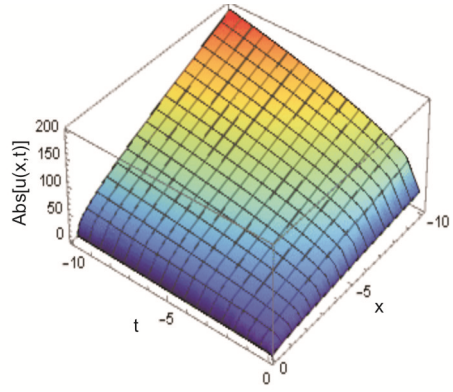

(a)

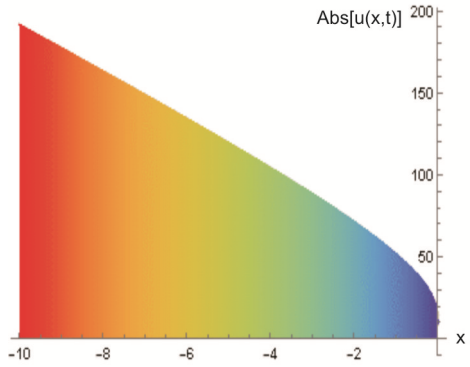

(b)

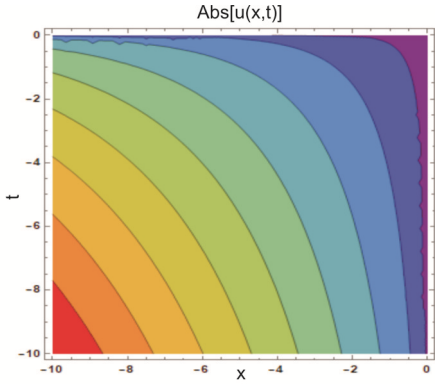

(c)

Fig. 18. Graph displays flat kink soliton of the modulus of the solution (48) for $a=2.9$, $b=2.5$, $k=0.9$, $n=1.9$, $\delta=-2$, $\beta=6$, $\vartheta=1$ and $\nu=0.24$: (a) 3D, (b) 2D, and (c) contour plot.

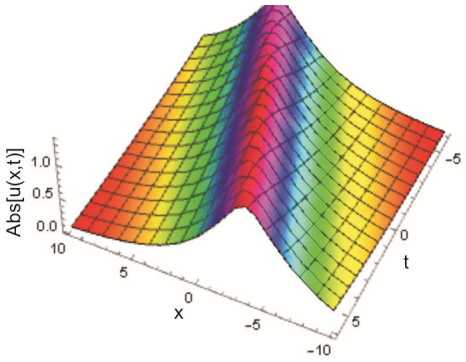

(a)

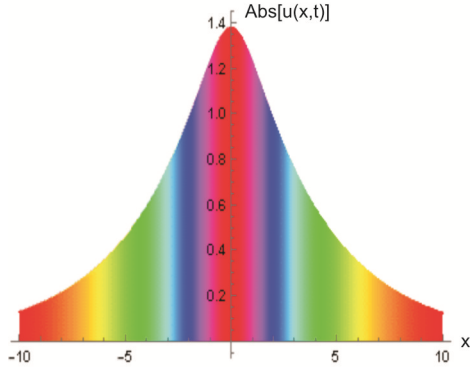

(b)

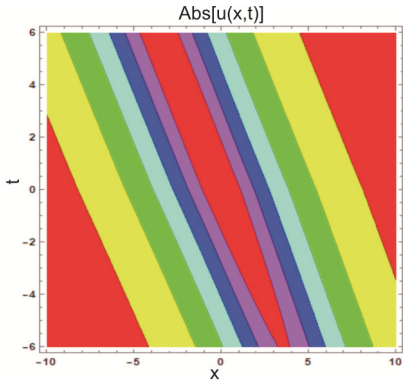

(c)

Fig. 19. Graph displays bell-shaped soliton of the modulus of the solution (48) for $a=3$, $b=2.5$, $k=0.1$, $n=1.9$, $\delta=-2$, $\beta=6$, $\vartheta=1$ and $\nu=0.99$: (a) 3D, (b) 2D, and (c) contour plot.

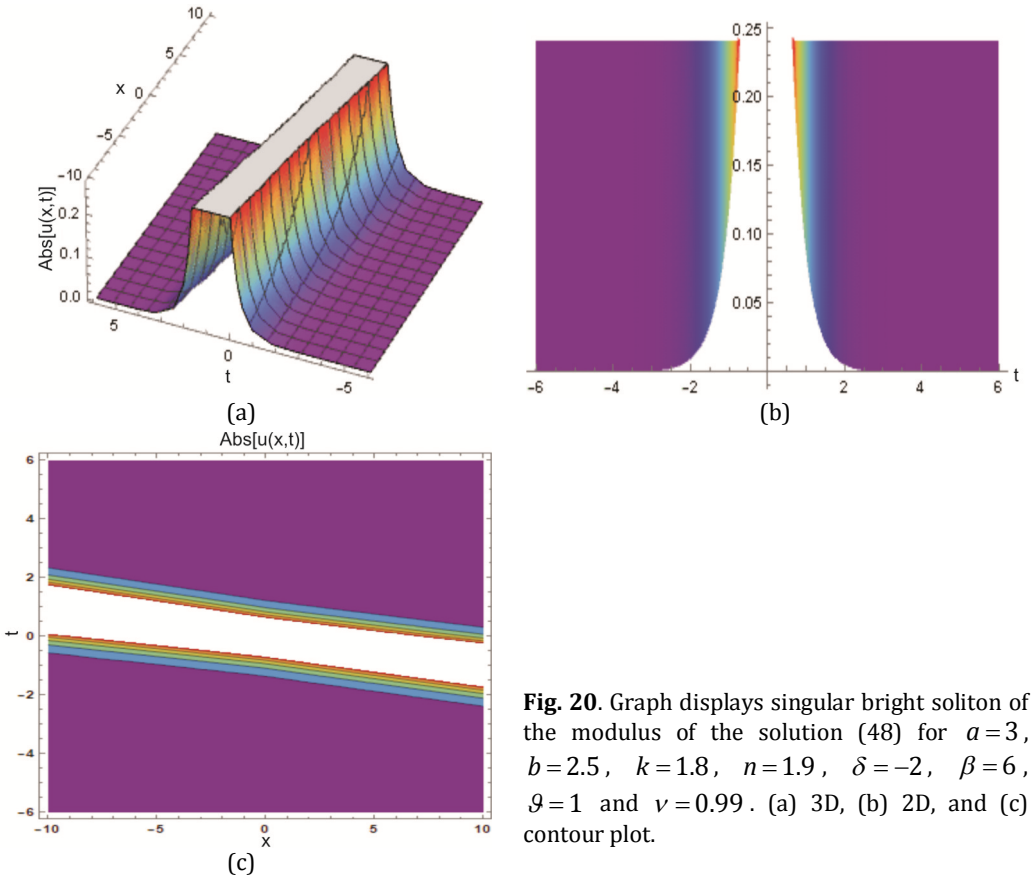

Fig. 20. Graph displays singular bright soliton of the modulus of the solution (48) for $a=3$, $b=2.5$, $k=1.8$, $n=1.9$, $\delta=-2$, $\beta=6$, $\vartheta=1$ and $\nu=0.99$. (a) 3D, (b) 2D, and (c) contour plot.

Based on the graphical analysis presented, it is evident that the soliton profile is predominantly influenced by the wavenumber *k*, the coefficients *ν* and *β* of two higher-order nonlinear dispersive terms, and the nonlinearity power *n*. The remaining parameters appear to exert minimal influence on the evolution of the wave structure.

Conclusion

In this article, we have thoroughly investigated the soliton dynamics of the generalized fractional nonlinear refractive index model and the fractional complex Ginzburg-Landau equation with power-law nonlinearity in optical systems. The sine-Gordon expansion approach within the conformable fractional derivative framework is used to establish a wide spectrum of exact soliton solutions for both models. The obtained waveforms demonstrate that changes in the fractional order, nonlinearity coefficients, and dispersion parameters strongly affect the soliton shape. These effects provide clear insight into how pulses can be modulated and controlled in dispersive and nonlinear media. The graphical analysis further clarifies the phase-amplitude interaction and highlights how fractional operators modulate wave structure in optical systems. The conformable derivative preserves standard properties of classical derivative, making physical interpretation easier, and it also introduces a scaling effect that allows more flexible modeling of non-integer-order processes. The results confirm that the SGE method is an effective analytical tool in optical wave applications. It reproduces several known solutions and also yields new types of solutions that enrich the existing solution structure.

In the future, this framework can be extended to other fractional operators, higher-dimensional models, or coupled nonlinear systems. Numerical simulations, stability analysis, and experimental validation in photonic and complex media in mathematical theory and physical applications are also the directions for future work.

Authorship contribution statement. Wael W. Mohammed: Resources, Software, Funding acquisition, Writing-Review Editing. Md. Tipu Sultan: Conceptualization, Resources, Methodology, Investigation, Data Curation, Visualization, Writing-Original Draft. Doaa Rizk: Investigation, Data Curation, Validation, Writing-Review Editing. M. Ali Akbar: Formal Analysis, Project administration, Supervision, Writing-Review Editing.

Declaration of competing interest. The authors declare that they have no known competing financial interests or personal relationships that could have appeared to influence the work reported in this paper.

Data availability. All data generated or analyzed during this study are included in this article.

Funding and acknowledgment. The researchers would like to thank the Deanship of Graduate Studies and Scientific Research at Qassim University for financial support (QU-APC-2026).

References

1. Darvishi, M. T., Najafi, M., & Wazwaz, A. M. (2021). Some optical soliton solutions of space-time conformable fractional Schrödinger-type models. *Physica Scripta*, *96*(6), 065213.
2. Akinyemi, L., Nisar, K. S., Saleel, C. A., Rezazadeh, H., Veeresha, P., Khater, M. M., & Inc, M. (2021). Novel approach to the analysis of fifth-order weakly nonlocal fractional Schrödinger equation with Caputo derivative. *Results in Physics*, *31*, 104958.
3. Ali, K. K., Osman, M. S., & Abdel-Aty, M. (2020). New optical solitary wave solutions of Fokas-Lenells equation in optical fiber via Sine-Gordon expansion method. *Alexandria Engineering Journal*, *59*(3), 1191-1196.
4. Yel, G., Bulut, H., & Ilhan, E. (2022). A new analytical method to the conformable chiral nonlinear Schrödinger equation in the quantum Hall effect. *Pramana*, *96*(1), 54.
5. Zulfiqar, A., & Ahmad, J. (2022). Dynamics of new optical solutions of fractional perturbed Schrödinger equation with Kerr law nonlinearity using a mathematical method. *Optical and Quantum Electronics*, *54*(3), 197.
6. Wang, L., Luan, Z., Zhou, Q., Biswas, A., Alzahrani, A. K., & Liu, W. (2021). Bright soliton solutions of the (2+ 1)-dimensional generalized coupled nonlinear Schrödinger equation with the four-wave mixing term. *Nonlinear dynamics*, *104*(3), 2613-2620.
7. Islam, M. E., & Akbar, M. A. (2020). Stable wave solutions to the Landau-Ginzburg-Higgs equation and the modified equal width wave equation using the IBSEF method. *Arab Journal of Basic and Applied Sciences*, *27*(1), 270-278.
8. Islam, M. T., Akter, M. A., Gómez-Aguilar, J. F., & Akbar, M. A. (2022). Novel and diverse soliton constructions for nonlinear space–time fractional modified Camassa–Holm equation and Schrodinger equation. *Optical and Quantum Electronics*, *54*(4), 227.
9. Mohammed, W. W., Iqbal, N., Sidaoui, R., & Ali, E. E. (2025). Dynamical behavior of the fractional nonlinear Kadoma equation in plasma physics and optics. *Modern Physics Letters B*, *39*(08), 2450434.
10. Rezazadeh, H., Ullah, N., Akinyemi, L., Shah, A., Mirhosseini-Alizamin, S. M., Chu, Y. M., & Ahmad, H. (2021). Optical soliton solutions of the generalized non-autonomous nonlinear Schrödinger equations by the new Kudryashov's method. *Results in Physics*, *24*, 104179.
11. Ali, E. E., Ennaceur, M., Mohammed, W. W., Algolam, M. S., & Ahmed, A. I. (2025). Investigation of New Optical Solutions for the Fractional Schrödinger Equation with Time-Dependent Coefficients: Polynomial, Random, Trigonometric, and Hyperbolic Functions. *Fractal and Fractional*, *9*(3), 142.
12. Obeidat, S. T., Ahmed, K. K., Ahmed, H. M., Mohammed, W. W., & Ghayad, M. S. (2025). Fractional derivative effects on exploration of soliton solutions of (3+ 1)-D Kadomtsev-Petviashvili-Sawada-Kotera-Ramani model using modified extended direct algebraic approach. *Contemp. Math*, *6*, 5346-5367.

13. Mohammed, W. W., Khatun, M. M., Algolam, M. S., Sidaoui, R., & Akbar, M. A. (2025). Analytical Solitary Wave Solutions of Fractional Tzitzéica Equation Using Expansion Approach: Theoretical Insights and Applications. *Fractal and Fractional*, *9*(7), 438.
14. Nikan, O., Molavi-Arabshai, S. M., & Jafari, H. (2021). Numerical simulation of the nonlinear fractional regularized long-wave model arising in ion acoustic plasma waves. *Discret. Contin. Dyn. Syst. S*, *14*(10), 3685-3701.
15. Nikan, O., & Avazzadeh, Z. (2021). An efficient localized meshless technique for approximating nonlinear sinh-Gordon equation arising in surface theory. *Engineering Analysis with Boundary Elements*, *130*, 268-285.
16. Rasoulizadeh, M. N., Ebadi, M. J., Avazzadeh, Z., & Nikan, O. (2021). An efficient local meshless method for the equal width equation in fluid mechanics. *Engineering Analysis with Boundary Elements*, *131*, 258-268.
17. Li, M., Nikan, O., Qiu, W., & Xu, D. (2022). An efficient localized meshless collocation method for the two-dimensional Burgers-type equation arising in fluid turbulent flows. *Engineering Analysis with Boundary Elements*, *144*, 44-54.
18. Safari, K., Rodriguez Vila, B., & Pierce, D. M. (2025). Automated detection of microcracks within second harmonic generation images of cartilage using deep learning. *Journal of Orthopaedic Research*, *43*(6), 1101-1112.
19. Arnous, A. H., Alqahtani, R. T., Ullah, M. Z., & Biswas, A. (2018). Dispersive optical solitons with DWDM technology by modified simple equation method. *Optoelectronics and Advanced Materials, Rapid Communications*, *12*(7-8), 431-435.
20. Arnous, A. H., Biswas, A., Ekici, M., Alzahrani, A. K., & Belic, M. R. (2021). Optical solitons and conservation laws of Kudryashov's equation with improved modified extended tanh-function. *Optik*, *225*, 165406.
21. Biswas, A., Yildirim, Y., Yasar, E., Triki, H., Alshomrani, A. S., Ullah, M. Z., ... & Belic, M. (2018). Optical soliton perturbation with full nonlinearity for Kundu–Eckhaus equation by modified simple equation method. *Optik*, *157*, 1376-1380.
22. Biswas, A., Ekici, M., Sonmezoglu, A., & Kara, A. H. (2019). Optical solitons and conservation law in birefringent fibers with Kundu–Eckhaus equation by extended trial function method. *Optik*, *179*, 471-478.
23. Zayed, E. M., Alngar, M. E., El-Horbaty, M., Biswas, A., Alshomrani, A. S., Khan, S., ... & Triki, H. (2020). Optical solitons in fiber Bragg gratings having Kerr law of refractive index with extended Kudryashov's method and new extended auxiliary equation approach. *Chinese Journal of Physics*, *66*, 187-205.
24. Zayed, E. M., Alngar, M. E., Biswas, A., Asma, M., Ekici, M., Alzahrani, A. K., & Belic, M. R. (2020). Solitons in magneto–optic waveguides with Kudryashov's law of refractive index. *Chaos, Solitons & Fractals*, *140*, 110129.
25. Zayed, E. M., Al-Nowehy, A. G., Alngar, M. E., Biswas, A., Asma, M., Ekici, M., ... & Belic, M. R. (2021). Highly dispersive optical solitons in birefringent fibers with four nonlinear forms using Kudryashov's approach. *Journal of Optics*, *50*(1), 120-131.
26. Yıldırım, Y., Biswas, A., Kara, A. H., Ekici, M., Alzahrani, A. K., & Belic, M. R. (2021). Cubic–quartic optical soliton perturbation and conservation laws with generalized Kudryashov's form of refractive index. *Journal of Optics*, *50*(3), 354-360.
27. El-Sheikh, M. M. A., Ahmed, H. M., Arnous, A. H., Rabie, W. B., Biswas, A., Alshomrani, A. S., ... & Belic, M. R. (2019). Optical solitons in birefringent fibers with Lakshmanan–Porsezian–Daniel model by modified simple equation. *Optik*, *192*, 162899.
28. Elsherbeny, A. M., El-Barkouky, R., Ahmed, H. M., Arnous, A. H., El-Hassani, R. M., Biswas, A., ... & Alshomrani, A. S. (2021). Optical soliton perturbation with Kudryashov's generalized nonlinear refractive index. *Optik*, *240*, 166620.
29. Murad, M. A. S. (2024). Optical solutions with Kudryashov's arbitrary type of generalized non-local nonlinearity and refractive index via the new Kudryashov approach. *Optical and Quantum Electronics*, *56*(6), 999.
30. Rizvi, S. T., Seadawy, A. R., & Akram, U. (2022). New dispersive optical soliton for an nonlinear Schrödinger equation with Kudryashov law of refractive index along with P-test. *Optical and Quantum Electronics*, *54*(5), 310.
31. Elsherbeny, A. M., Elsonbaty, N. M., Badra, N. M., Ahmed, H. M., Mirzazadeh, M., Eslami, M., ... & Bayram, M. (2024). Optical solitons of higher order mathematical model with refractive index using Kudryashov method. *Optical and Quantum Electronics*, *56*(6), 935.
32. Fahad, A., Boulaaras, S. M., Rehman, H. U., Iqbal, I., Saleem, M. S., & Chou, D. (2023). Analysing soliton dynamics and a comparative study of fractional derivatives in the nonlinear fractional Kudryashov's equation. *Results in Physics*, *55*, 107114.

33. Murad, M. A. S., Arnous, A. H., Faridi, W. A., Iqbal, M., Nisar, K. S., & Kumar, S. (2024). Two distinct algorithms for conformable time-fractional nonlinear Schrödinger equations with Kudryashov's generalized non-local nonlinearity and arbitrary refractive index. *Optical and Quantum Electronics*, *56*(8), 1320.
34. Doering, C. R., Gibbon, J. D., Holm, D. D., & Nicolaenko, B. (1988). Low-dimensional behaviour in the complex Ginzburg-Landau equation. *Nonlinearity*, *1*(2), 279-309.
35. Weitzner, H., & Zaslavsky, G. M. (2003). Some applications of fractional equations. *Communications in Nonlinear Science and Numerical Simulation*, *8*(3-4), 273-281.
36. Al-Ghafri, K. S. (2020). Soliton behaviours for the conformable space–time fractional complex Ginzburg–Landau equation in optical fibers. *Symmetry*, *12*(2), 219.
37. Huang, C., & Li, Z. (2021). New exact solutions of the fractional complex Ginzburg–Landau equation. *Mathematical Problems in Engineering*, *2021*(1), 6640086.
38. Akram, G., Arshed, S., Sadaf, M., & Farooq, K. (2023). A study of variation in dynamical behavior of fractional complex Ginzburg-Landau model for different fractional operators. *Ain Shams Engineering Journal*, *14*(9), 102120.
39. Siddique, I., Mehdi, K. B., Eldin, S. M., & Zafar, A. (2023). Diverse optical solitons solutions of the fractional complex Ginzburg-Landau equation via two altered methods. *Applied Mathematics for Modern Challenges*, *8*(5).
40. Leta, T. D., Chen, J., & El Achab, A. (2023). Innovative solutions and sensitivity analysis of a fractional complex Ginzburg–Landau equation. *Optical and Quantum Electronics*, *55*(10), 931.
41. Murad, M. A. S., Ismael, H. F., Hamasalh, F. K., Shah, N. A., & Eldin, S. M. (2023). Optical soliton solutions for time-fractional Ginzburg–Landau equation by a modified sub-equation method. *Results in Physics*, *53*, 106950.
42. Akram, G., Sadaf, M., & Mariyam, H. (2022). A comparative study of the optical solitons for the fractional complex Ginzburg–Landau equation using different fractional differential operators. *Optik*, *256*, 168626.
43. Zafar, A., Shakeel, M., Ali, A., Akinyemi, L., & Rezazadeh, H. (2022). Optical solitons of nonlinear complex Ginzburg–Landau equation via two modified expansion schemes. *Optical and Quantum Electronics*, *54*(1), 5.
44. Sadaf, M., Akram, G., & Dawood, M. (2022). An investigation of fractional complex Ginzburg–Landau equation with Kerr law nonlinearity in the sense of conformable, beta and M-truncated derivatives. *Optical and Quantum Electronics*, *54*(4), 248.
45. Ismael, H. F., Bulut, H., & Baskonus, H. M. (2020). Optical soliton solutions to the Fokas–Lenells equation via sine-Gordon expansion method and (m+(G′/G))-expansion method. *Pramana*, *94*(1), 35.
46. Ananna, S. N., An, T., Asaduzzaman, M., & Rana, M. S. (2022). Sine-Gordon expansion method to construct the solitary wave solutions of a family of 3D fractional WBBM equations. *Results in Physics*, *40*, 105845.
47. Kumar, D., Hosseini, K., & Samadani, F. (2017). The sine-Gordon expansion method to look for the traveling wave solutions of the Tzitzéica type equations in nonlinear optics. *Optik*, *149*, 439-446.
48. Korkmaz, A., Hepson, O. E., Hosseini, K., Rezazadeh, H., & Eslami, M. (2020). Sine-Gordon expansion method for exact solutions to conformable time fractional equations in RLW-class. *Journal of King Saud University-Science*, *32*(1), 567-574.
49. Kayum, M. A., Ara, S., Osman, M. S., Akbar, M. A., & Gepreel, K. A. (2021). Onset of the broad-ranging general stable soliton solutions of nonlinear equations in physics and gas dynamics. *Results in Physics*, *20*, 103762.
50. Darvishi, M. T., Najafi, M., & Wazwaz, A. M. (2021). Conformable space-time fractional nonlinear (1+ 1)-dimensional Schrödinger-type models and their traveling wave solutions. *Chaos, Solitons & Fractals*, *150*, 111187.
51. Khalil, R., Al Horani, M., Yousef, A., & Sababheh, M. (2014). A new definition of fractional derivative. *Journal of Computational and Applied Mathematics*, *264*, 65-70.

Mohammed, W. W., Sultan, Md. T., Rizk, D., Ali Akbar, M. (2026). Soliton Propagation, Modulation, and Stability Analysis of Fractional Nonlinear Optical Models: A Conformable Derivative Approach**.** *Ukrainian Journal of Physical Optics*, *27*(3), 03041 – 03068.
doi: 10.3116/16091833/Ukr.J.Phys.Opt.2026.03041

Анотація. *У цій статті ми встановлюємо широкий клас точних солітонних розв'язків узагальненого нелінійного рівняння показника заломлення Кудряшова та дробового комплексного рівняння Гінзбурга-Ландау. Дробова похідна забезпечує узагальнену математичну основу для моделювання складних дисперсійних та нелінійних ефектів в оптичних середовищах. Її точні розв'язки допомагають зрозуміти якісні особливості поширення хвиль, такі як стабільність та локалізація. Структура конформних*

похідних підтверджує математичну надійність та фізичну застосовність при моделюванні дисперсії дробового порядку та нелінійних ефектів. Підхід розкладання синус-Гордона (SGE) використовується в рамках структури конформних дробових похідних для систематичного аналізу моделей. Цей підхід дає широкий спектр аналітичних розв'язків, включаючи дзвоноподібні, антидзвіноподібні, кінкові, бризерні, гострі, W-подібні, параболічні та сингулярні солітони. Результати показують, що параметри хвилі, такі як частота хвилі, форма солітона та амплітуда, добре описуються дробовим порядком α. Вони дають уявлення про поширення імпульсів та характеристики форми хвилі в нелінійних середовищах. Графічні представлення, включаючи дво- та тривимірні та контурні візуалізації, ілюструють амплітуду, фазову взаємодію та структурні переходи між сімействами солітонів. Це дослідження демонструє, що підхід SGE ефективно генерує точні розв'язки для дробово-нелінійних еволюційних рівнянь, що стосуються нелінійної волоконної оптики та інших систем зі складними хвильовими взаємодіями.

Ключові слова: *дробова похідна, моделювання, оптичні солітони, нелінійний показник заломлення, комплексне рівняння Гінзбурга-Ландау, метод розкладу синус-Гордона*